Topology Optimization of Plates

B. Boroomand
A. R. Barekatein

Publication CIMNE Nº-298, December 2006

Topology Optimization of Plates

B. Boroomand
A. R. Barekatein

Publication CIMNE Nº-298, December 2006

International Center for Numerical Methods in Engineering
Gran Capitán s/n, 08034 Barcelona, Spain

Topology Optimization of Plates

B. Boroomand and A.R. Barekatein

Civil Engineering Department, Isfahan University of Technology, Isfahan 84156-83111, Iran

Email: boromand@cc.iut.ac.ir

Abstract

In this report we propose a stabilization method for topology optimization of plates. The method can be classified in the category of continuation methods. The new continuation method is based on using continuous fields of design variables (DV) defined on a set of meshes different from the one used for the finite element solution. The optimization procedure starts with using a coarse DV-mesh compared to finite element one. Once the convergence is obtained in the optimization steps, a finer DV-mesh is nominated for further steps. With such a continuation method one can control the bounds of the gradients of the DV while simultaneously smooth the values in a more logical fashion, compared to what conventional filters perform. The DV-mesh refinement can be continued until the final mesh becomes similar to the finite element mesh. Depending on the formulation and elements used for the plate problems, e.g. with Kirchhoff or Mindlin-Reissner hypothesis, the refinement may further be continued so that the DV elements become smaller than the plate elements. Application of the method is shown over a wide range of plate problems. Linear and nonlinear plate behaviors formulated by Kirchhoff or Mindlin-Reissner hypothesis, while using several forms of DV, are considered to show the performance of the proposed method. As one of the main DV, density is used in a power-law approach (or in an artificial material approach). This is performed in two forms, one in obtaining the topology of a perforated plate-like structure and another in determining the topology of the plate stiffeners. Thickness is also used as a realistic design variable in order to show the performance of the method in a rather well-posed optimization problem. We have also included results from a homogenization approach. Comparison is made with conventional element/nodal based approaches using filter. The results show excellent and robust performance of the proposed method. Due to the wide range of cases studied, some inserting side conclusions are also given in this report.

Keywords: *Topology optimization, plate, continuation, stabilization, refinement, mesh dependency, checkerboard*

Contents

1. INTRODUCTION

From introduction of the Finite Element based topology optimization by Bendsøe and Kikuchi (1988) and Bendsøe (1995) the method has so far received a considerable amount of attention by many researchers. The reason is clearly its wide range of applications in engineering.

In essence, the problem in topology optimization is finding an optimal structural design from a primitive continuum. Like many other optimization methods different objective functions, design variables (DV), constraints and even mathematical programming schemes may be used. Finite element method is usually used as the solution tool and the distribution of the DV is determined through discrete values defined over the elements. The optimization procedure continues until a clear topology, i.e. black and white one representing regions with maximum and minimum values of the variable, is obtained. The history of different approaches can be found in the recent review paper by Rozvany (2001). Most of the studies have been devoted to linear problems.

The method has also been employed in nonlinear problems. Few researches can be traced in the literature for this class of problems. For structures with material nonlinearity, contributions by Bendsøe *et al.* (1995), Swan and Kosaka (1997) and Maute *et al.* (1998) should be mentioned here. For structures with large displacements, studies by Jog (1997), Bruns and Tortorelli (1998, 2001), Cho and Jung (2003), Buhl *et al.* (2000) and Pedersen *et al.* (2001) are notable ones.

In most of the studies, it has been concluded that the optimal designs in linear and nonlinear cases are almost identical until the structure undergoes a very large displacement (e.g. see Cho and Jung (2003), Buhl *et al.* (2000) and Pedersen *et al.* (2001)). The studies have focused on topologies of two dimensional structures with in-plane loadings.

Apart from the differences/similarities between topologies obtained due to linear/nonlinear behavior or due to using different optimization procedures, in some circumstances the numerical solution suffers from a non-uniqueness effect. Mesh dependency of the results and the problem of obtaining checkerboard patterns are the consequences of such an effect. This of course may depend on the choice of DV. For example in two dimensional elasticity problems when minimization of compliance is of concern and the dimensions of micro-holes are considered as the DV, the solution may lack the uniqueness property. This is because, in a mathematical point of view, the optimal solution may consist of some regions with infinite number of infinitesimal holes and thus the layout may not be captured by refining the elements. Such an effect is sometimes referred to as ill-posed-ness of the problem. However, the same problem may show uniqueness when thickness of the points is considered as the DV. Nevertheless, even in this latter case if the DV field is defined by a series of discontinuous values over the elements, the problem of checkerboard pattern may encounter because of the over stiffness effect of the pattern.

The effects of checkerboard and mesh dependency are seen in almost all commonly used approaches for topology optimization, i.e. use of homogenization method pioneered by Bendsøe and Kikuchi (1988) and the use of artificial materials pioneered by Bendsøe (1989) and Rozvany and Zhou (1991) (see also the review by Bendsøe (1995)). The effects become severe when penalization factors are used for the intermediate values of DV.

Several remedies have so far been suggested by scientists. The remedies can mainly be categorized in; those using restriction methods and those using continuation methods. Methods using restrictions on perimeter of the holes or on the gradients of the variables Haber et al 1996, Petersson (1999) or Niordson (1983), Petersson and Sigmund (1998) are among the first category and those utilizing filters Sigmund (1994), Sigmund and Petersson (1998), Bourdin (2001), Pedersen (2001) are among the second one.

On the same line, other researchers focus on using continuous fields of DV instead of discontinuous ones. In fact the motive lies in the mathematical model of the optimization problem for which the

uniqueness of the solution is sometimes possible to be proved when the variables are considered continuous across the design domain. The first thought is traced in the work by Jog and Haber (1996) in which the formulation of topology optimization was cast in the framework of mixed variational problems. Thickness was considered as the DV in two dimensional plane problems.

From the literature it appears that continuous fields of DV have extensively been used by Rahmatalla and Swan (2003, 2004). In the second paper, using density as the design variable, the authors examine a series of low and high order elements for finite element solution while interpolating the DV. They recommend the use of linear rectangular elements for both analysis and design domains. Their studies show that a sort of instability, called "layering" effect, is still seen in the optimal layout which is in fact a mesh-dependent effect. Such a combination of elements was also examined through the patch tests introduced by Jog and Haber (1996). The tests indicate that such a combination may lead to unstable results.

In the studies by Matsui and Terada (2004), the dimensions and orientation of holes, in a homogenization scheme, were considered as the DV. In a rather similar manner to the work by Rahmatalla and Swan (2004), in this latter work continuous fields of DV were built through interpolation of the nodal values defined at the nodes where the corners of the elements are met. The approach still suffers form the mesh dependency effect. Use of some additional restrictions was recommended by the authors of the paper.

The above mentioned studies are basically on two dimensional plane problems (especially linear ones). Since the principles of the formulation in two and three dimensional problems are similar, it is expected that the same effects be seen in the solution of three dimensional problems and thus similar remedies be applicable. However, for some special two dimensional problems like plate problems, where the formulation is derived by specific assumptions from a general three dimensional one, the effect of instability in the solution may become more severe. This may become worse when nonlinear solution is of concern in plates.

Few studies can be found in literature for topology optimization of plates. This seems to be due the fact that the problem is much more ill-posed compared to two/three dimensional ones especially when through-thickness holes are considered to obtain the topology. Such a difficulty is alleviated when the topology of layers in a composite plate is of concern. In this latter case the thin layers in fact behave as two dimensional plane problems. Studies by Maute and Ramm (1997) and Pedersen (2001) and Kemmler *et* al (2005) fall within the first category of approaches and those by Lee *et al* (2000) and Stegmann and Lund (2004) fall in the second category of approaches. In most of these studies, especially when artificial materials are employed, the use of one of the continuation methods has been recommended.

In this report we shall focus on plate problems since on one hand these problems are more sensitive with respect to convergence, mesh dependency and checkerboard effects and on the other hand they can indirectly reflect the behavior of two dimensional plane problems when they are used in layered forms. We shall show that mesh dependency and obtaining checkerboard patterns are severe problems in topology optimization of plates especially in linear cases. Both linear and non-linear behaviors will be considered. To alleviate the instability effects we shall use continuous fields of DV. To the best knowledge of the authors this is the first study on the use of such continuous fields for plate problems. As will be seen in this report, use of continuous fields, solely, does not reduce the mesh dependency problem. Here we propose a continuation method which is consistent with some restriction methods, i.e. gradient restriction, and other continuation methods like those use filters. In the proposed approach a series of meshes are used for interpolation of DV. During the optimization the finite element solution is performed on a separate fine mesh while changing the DV mesh from the coarse one to the fine one in a sequential manner. We call the method as Node-based Design with Enhancive Resolution (NDER). Like other continuation methods there may be no rigorous mathematical justification for the method we

propose. However, to demonstrate that the method works for many cases, variety of DV together with two well known plate formulations, i.e. formulation with Kirchhoff or Mindlin assumptions for both linear and nonlinear behaviors, are considered here. Apart from demonstration of the results for the convergence, the topologies obtained from different hypothesis and DV are used to draw useful side conclusions.

It appears that the idea of using successive meshes in topology optimization of 2-D problems is being addresses by other scientists (see the parallel and very recent work by Stolpe and Stidsen (2006)). In their work, Stolpe and Stidsen proposed a mathematical programming approach in which the feasible domain is found through the use of macro-elements with 0-1 material density (with no material-or fully filled with material). The aspect of the present work is different form their work in two basic features. The first one is that we shall use a continuous field for the DV (also note that the DV here is more general than those proposed by Stolpe and Stidsen) rather than a discontinuous one. This enables us to control the gradient of the DV, as will be discussed later, throughout the optimization process. As suggested in their paper, Stolpe and Stidsen still need a suitable checkerboard control algorithm during the process, and this is because of the discontinuous density field used, while the effect is assumed to be controlled inherently in our approach since the interpolation we use acts as a replacement for the filters usually employed (see the paper by Sigmund (1994)). The second one is that with our approach one can use conventional mathematical programming methods. Here we shall use wildly accepted mathematical programming, i.e. the Method of Moving Asymptotes, proposed by Svanberg (1987, 2002).

In the context of using progressive resolution in the topology optimization, the work by Kim and Yoon (2000) should be mentioned here. In their studies, Kim and Yoon use a wavelet based design and improve the resolution by reducing the supports of the wavelet basis, as well as increasing the number of them, during the procedure. The study has been performed on two dimensional plane problems. As they mentioned in the paper, the side constraints are not satisfied conveniently due the fact that an intermediate space is used to define the DV (in this case density). As will be seen later in this report, our approach is different form theirs in the sense that, firstly, we basically use shape functions for defining a continuous field of DV. This is very consistent with the finite element formulation and may be interpreted as an indirect mixed formulation (see Zienkiewicz and Taylor (2000) for general mixed formulation and Jog and Haber (1996) for interpretation of nodal based design as the mixed formulation). This makes the formulation very simple and most probably may provide the opportunity of performing more comprehensive studies in a similar manner as performed for the general formulation in this kind. Secondly, by controlling the nodal values of DV during optimization one may easily apply the side constraints. Also there will be no need for introducing new intermediate variables in the available mathematical programming algorithms.

The layout of the report is as follows; in the next section we overview the plate formulation. We start with nonlinear formulation since the linear one may be considered as a special case. Both thin and thick plate formulations are revisited since the paths towards optimal solution may differ. We have also included formulation for laminated plates to give an indirect insight to the capability of the method for solution of simple two dimensional plane problems. In Section 3 the general statement of the optimization problem is given. In the same section we address the use of several choices of DV along with the details of the proposed method. Section 4 is devoted to numerical results and the discussions on a wide range of examples. We shall summarize the conclusions in the final part of the report.

2. MODEL PROBLEM

In this section we shall overview the essential parts of the mathematical model used in this report. We commence with nonlinear formulation. However, in the section of numerical examples we shall give some results on linear problems whose formulation is covered by nonlinear cases.

Considering that the structure undergoes a relatively large deflection, the plate formulation starts from

Green-Lagrange strain measure as

$$E_{ij} = \frac{1}{2}\left(u_{i,j} + u_{j,i} + u_{k,i}u_{k,j}\right) \tag{1}$$

Here u_i denotes a generic displacement component in a three dimensional space. In the case that the plate is sufficiently thin, the components of displacement field can be degenerated from a three dimensional form by some appropriate assumptions. The displacement components are then written as

$$\mathbf{u} = \begin{Bmatrix} u_1 \\ u_2 \\ u_3 \end{Bmatrix} = \begin{Bmatrix} u_{(x,y)} \\ v_{(x,y)} \\ w_{(x,y)} \end{Bmatrix} - z \begin{Bmatrix} \theta_x \\ \theta_y \\ 0 \end{Bmatrix} \tag{2}$$

Where θ_x and θ_y are the components of the rotation at a point.

Assuming that the in-plane deformations are small and the deflection is within the order of the thickness, as von-Karman type of assumptions, one can rewrite Equation (1) in a matrix form as

$$\mathbf{E} = \mathbf{E}^p - z\mathbf{K}^b \tag{3}$$

where $\mathbf{E}^p$ is a part pertaining to in-plane strains and $\mathbf{K}^b$ contains the components of the rotation in an appropriate arrangement.

In the equilibrium state, the induced stresses must satisfy the principles of virtual work. In view of (3) following equation can be written for virtual work

$$\delta\Pi = \int_\Omega \left(\delta\mathbf{E}\right)^T \mathbf{S}\, d\Omega - \delta\Pi_{ext} = \mathbf{0} \tag{4}$$

where $\mathbf{S}$ denotes the vector of the second Piola-Kirchhoff stresses arranged in a similar manner as $\mathbf{E}$ in (3), $\delta\Pi_{ext}$ represents the virtual work of external forces and Ω is the plate volume.

In topology optimization, plates are considered to be reasonably thin. The term "thin" in plate problems is usually used when the dimensions of the plate are more than 10 times of the thickness. However in the process it happens that in some small regions, an e.g. near corner of the perforated structure, this limitation is not met. In almost all studies in this kind available in the literature, shear deformable formulation have been used, i.e. formulations based on Mindlin-Reissner hypothesis. Nevertheless, in this report we show that formulations without shear deformability assumption for the plate, i.e. formulation with Kirchhoff hypothesis, give similar results.

In this section we briefly overview both formulations, firstly to show the differences when different DV are used and secondly to demonstrate the performance of the proposed method.

2.1 Formulation by Kirchhoff hypothesis

Neglecting shear deformations, one may assume

$$\theta_x = \frac{\partial w}{\partial x} = w_{,x}\,,\ \theta_y = \frac{\partial w}{\partial y} = w_{,y} \tag{5}$$

This helps to write $\mathbf{K}^b$ in terms of second derivatives of the deflection. Equation (4) can now be written in the following form

$$\int_A \left(\delta\mathbf{E}^{pb}\right)^T \mathbf{S}^{pb}\, dA - \delta\Pi_{ext} = \mathbf{0} \tag{6}$$

In which A is the plate area. Also

$$\delta\mathbf{E}^{pb}=\begin{Bmatrix}\delta\mathbf{E}^{p}\\ \delta\mathbf{K}^{b}\end{Bmatrix},\ \mathbf{S}^{pb}=\begin{Bmatrix}\mathbf{T}^{p}\\ \mathbf{M}^{b}\end{Bmatrix} \tag{7}$$

where the components of the stress resultants and the associated strains are related as

$$\mathbf{T}^{p}=\mathbf{D}^{p}\mathbf{E}^{p},\ \mathbf{M}^{b}=\mathbf{D}^{b}\mathbf{K}^{b} \tag{8}$$

In above relations $\mathbf{T}^{p}$ and $\mathbf{M}^{b}$ denote vectors of the in-plane and the bending stress resultants, respectively.

Assuming plane stress condition for the plate problem, the moduli for membrane and flexural behavior are in the form of

$$\mathbf{D}^{p}=t\,\mathbf{d},\ \mathbf{D}^{b}=\frac{t^{2}}{12}\mathbf{D}^{p},\ \mathbf{d}=E\begin{bmatrix}d_{11}&d_{12}&0\\ d_{21}&d_{22}&0\\ 0&0&d_{33}\end{bmatrix} \tag{9}$$

In above E is the Young's modulus and t is the plate thickness. For isotropic-homogenized materials the following relations exist between the elements of $\mathbf{d}$

$$d_{11}=d_{22},\ d_{12}=d_{21},\ d_{33}=\frac{d_{11}-d_{12}}{2} \tag{10}$$

For a real isotropic material well known relations as $d_{11}=d_{22}=\left(1-\nu^{2}\right)^{-1}$, $d_{12}=d_{21}=\nu/\left(1-\nu^{2}\right)$ and $d_{33}=\left[2\left(1+\nu\right)\right]^{-1}$, with ν being the Poisson's ratio of the material, exist. However, for artificially homogenized materials or laminated materials the definitions of elements of $\mathbf{d}$ may be different. Note that in (9) no coupling term has been considered between normal stresses and shear stress. This inherently means that in this report the homogenization, wherever used, is performed so that the material remains isotropic.

Depending on the approach used for the optimization part, either E or other components may be considered variable with respect to the density or the void ratio of the material during the procedure. Clearly the paths of optimizations toward optimal topology will be different. This can affect either the configuration of the final solution or the convergence of the procedure and in fact is one of the aspects of the current study.

2.2 Formulation by Mindlin-Reissner hypothesis

Similar expressions are obtained by Mindlin-Reissner hypothesis with the main difference that the components of rotation are considered as independent variables. The differences between the gradients of the deflection and the components of rotation are considered as measures for shear deformation across the thickness. Therefore the following vector is defined

$$\boldsymbol{\varepsilon}^{s}=\begin{Bmatrix}w_{,x}-\theta_{x}\\ w_{,y}-\theta_{y}\end{Bmatrix} \tag{11}$$

Such assumptions are sometimes referred to as first order shear deformation theory of plates (see Simo and Fox (1989) for higher order formulation).

Now with such a definition for shear deformations, the virtual work equation can be written as

$$\int_{A}\left(\delta\mathbf{E}^{psb}\right)^{T}\mathbf{S}^{psb}dA-\delta\Pi_{ext}=\mathbf{0} \tag{12}$$

Here again A is the area of the plate. In the above relation

$$\delta\mathbf{E}^{psb}=\begin{Bmatrix}\delta\mathbf{E}^{p}\\ \delta\boldsymbol{\varepsilon}^{s}\\ \delta\mathbf{K}^{b}\end{Bmatrix},\ \mathbf{S}^{psb}=\begin{Bmatrix}\mathbf{T}^{p}\\ \mathbf{T}^{s}\\ \mathbf{M}^{b}\end{Bmatrix} \tag{13}$$

where the components of stress resultants and the associated strains are related as

$$\mathbf{T}^{p}=\mathbf{D}^{p}\mathbf{E}^{p},\ \mathbf{T}^{s}=\mathbf{D}^{s}\boldsymbol{\varepsilon}^{s},\ \mathbf{M}^{b}=\mathbf{D}^{b}\mathbf{K}^{b} \tag{14}$$

Again assuming plane stress conditions for the plate problem, the moduli for membrane and flexural behavior will be in the form of (9) but the shear modulus is written as

$$\mathbf{D}^{s}=\left(\alpha E\, d_{33}\, t\right)\begin{bmatrix}1 & 0\\ 0 & 1\end{bmatrix} \tag{15}$$

where α is a shear correction factor (in this report is taken as $5/6$). Here again it can be seen that different approaches for topology optimization may lead to different paths towards optimal solution (even in the case of small stains with linear solution).

2.3 Laminated plates (plates with stiffeners)

Laminated plates are sometimes used for topology optimization. In that case the layouts of the laminas, rather than the layout of the plate, are determined during the optimization procedure. In its simplest form, this in fact is similar to optimization of the plate stiffeners. An example is the optimal layout of the reinforcements of a concrete slab. In this report we shall give some results on optimal topology of laminated plates in order to cover more cases for examining the performance of the proposed method.

Similar assumptions used in the preceding subsections can be made here to formulate the problem. However, when the thicknesses of the lamina are considerable, compared to the thickness of the plate (laminate), higher order deformation theories should be employed. The reader may refer to references Simo and Fox (1989) for higher order deformation theories in beams, plates and shells.

Nevertheless, in topology optimization of plates it is usually assumed that few laminas are used and their thicknesses are small enough to use first order deformation theories (see for instance Jones 1999). Therefore, the formulation of laminated plates is basically similar to those given above but of course the matrices of material modulus are different.

In this report we shall just use Kirchhoff hypothesis for formulation of the laminate, i.e. we shall follow the classical theory of laminate explained in Jones 1999. (The reader may note that using Mindlin-Reissner hypothesis for such a problem needs a shear correction factor which is dependent on the height and stiffness of the layers used). Also, we shall use just a three layer symmetric laminate model. In such a laminate two materials are needed to be chosen, one as the main/filler and another as two layers of stiffeners. Here, we aim at giving optimal layout of the stiffener material. The materials are considered to be isotropic and thus one can define two matrices for material constants as

$$\mathbf{d}_{i}=E_{i}\begin{bmatrix}d_{11}^{i} & d_{12}^{i} & 0\\ d_{21}^{i} & d_{22}^{i} & 0\\ 0 & 0 & d_{33}^{i}\end{bmatrix},\ i=1,2 \tag{16}$$

Now supposing that the first lamina, with height of h, plays the role of the filler and the second one, in two layers each with thickness of t_s, plays the role of stiffeners, the moduli for membrane an flexural behaviors (in-plane an bending actions) of the laminate can be written as

$$\mathbf{D}^p = h\,\mathbf{d}_1 + 2t_s\mathbf{d}_2\,,\ \mathbf{D}^b = \frac{1}{12}\left\{h^3\mathbf{d}_1 + \left[\left(h+2t_s\right)^3 - h^3\right]\mathbf{d}_2\right\} \tag{17}$$

The rest of the formulation is as those given in (6) to (8).

3. OPTIMIZATION PROBLEM

Optimal topology of structures can nowadays be attained by a number of approaches. The homogenization method introduced by Bendsøe and Kikuchi (1988) may be employed to obtain a layout for optimal distribution of orthotropic microstructures. In that case, the final optimal layout consists of a series of perforated elements. A hole as large as an element represents a region with no material and an element with no hole represents a region fully filled with material. Intermediate cases may also happen when the element is partially filled with the material. These intermediate cases, although have physical meaning, are difficult to manufacture.

Several other approaches have been employed by researchers and a good survey to the date can be found in the papers by Rozvany (2001), and Eschenauer and Olhoff (2001). One of the most effective and simple approaches recently employed by many researchers is called Solid Isotropic Microstructure with Penalization (SIMP). It appears that the idea was formed in early 1990s at rather the same time by Bendsøe and Rozvany, independently. The basic idea is to relate material modulus to power of the density of the material. For this reason the approach has also been called as "Power-law" method. The material remains isotropic during the optimization process. Intermediate densities are penalized by choosing appropriate power for the density and therefore it is expected that the layout of the optimal design of the material be in the form of black-white patterns. However some authors cast doubt on meaningfulness of the material for manufacturing of the design obtained. Investigation through an inverse homogenization approach by Bendsøe, and Sigmund (1999) shows that the model can be realizable if the power used is more than three and the Poisson's ratio of the material is equal to one third.

One of the realizable cases for SIMP is when the power equals to unity. For two-dimensional plane stress/strain problems it can easily be shown that such a case is equivalent to the use of thicknesses of the elements as the DV. However, this is not true for layout optimization in plate problems with out of plane loads. In fact for elastic plates with infinitesimal strain deformations the use of power equal to three is equivalent to the use of thickness as the DV. Nevertheless, for plates with nonlinear behavior no unique power can be specified for the equivalence between the two cases.

In this report we shall use the SIMP or "power-law" method as the main approach. Nevertheless, we shall give some examples on use of homogenization method where we assume that the material remains isotropic during the optimization. This helps us to compare the results with those obtained with SIMP method.

Since the problem can be nonlinear, we shall also examine the use of thickness of the plate as the design variable which is obviously different from the use of power-law method with the power equal to unity or three.

In any of the cases mentioned, the optimization procedure can be summarized as finding a minimum for an objective function like f, to be specified later, such that

$$\begin{aligned} &\text{Minimize: } f\left(\gamma\right) \\ &\text{Subject to: Equality constraint, } \quad \Psi = 0 \qquad (18) \\ &\qquad \text{and side constraint} \begin{cases} \int \gamma dA \le M \\ \gamma_{\min} \le \gamma \le \gamma_{\max} \end{cases} \end{aligned}$$

where γ denotes the design variable (DV), $\gamma_{\min}$ and $\gamma_{\max}$ are lower and upper bounds of the variables. Also, in above M represents the maximum allowable norm of the variables, e.g. total mass or volume of the material. In a numerical approach, the DV field is considered as a series of discrete values.

3.1 The design variables (DV) used

Having defined the objective functions, one may still obtain different layouts for optimal design when different variables are used.

Thicknesses as the design variables

Since the plate thickness is one of the shape parameters of the problem, the approach is sometimes categorized in shape optimization methods. In using thickness as the DV, we use $\gamma = t$ in (18). In that case M denotes total volume of material used.

Density as the design variable

As discussed earlier, the density of material is used as the DV in a wide range of recent studies. We shall use the concept in two forms, i.e. SIMP and homogenization formulations.

- *The SIMP (or power law) method*

In this form, the Young's modulus of material is expressed in terms of a power of the material density,

$$E = E_0 \rho^m \tag{19}$$

where E_0 is a base modulus and ρ is the density value (mass per unit area of the plate). Note that the Poisson's ratio is considered to be fixed (e.g. $\nu = \frac{1}{3}$ in this study).

For plate problem it has been recommended that linear variation be considered for Young's modulus when the density value becomes less than a specified value (see Pederson (2001) for example). Thus

$$E = E_0 \frac{1}{\sqrt{20}} \rho \quad \text{for} \quad \rho \le \rho_{thresh} \tag{20}$$

This helps to avoid numerical instabilities when the density takes very low values. However, when a minimum stiffness is considered for the plate, for instance in the case of finding topology of the stiffeners, there is no need for considering such a threshold value.

- *The homogenization method*

In this form, homogenous materials are considered in place of the perforated ones during the optimization process. For such replacements, the microstructure configuration is assumed to be periodic at the vicinity of the material point. This assumption leads to a simple averaging technique for evaluation of the homogenized material properties. The procedure can be found in the literature, see Bendsøe and Kikuchi (1988) and the review paper by Hassani and Hinton (1998).

In this report we assume that the microstructure configuration is so that the homogenized material is isotropic. Several configurations may be considered for such a purpose. Here, we consider two models for the microstructures. The first one is used for thin plate theory with a though-thickness hole for the sheet (see Figure 1-a). In this form we basically deal with a generic two-dimensional isotropic microstructure. The model has been used by some other researchers (see Tenek and Hagiwara (1993)). The second model, as shown in Figure 1-b, is used for thick plate theory. The microstructure in this model consists of a cube of material with an inner cubic hole. In this case the homogenized material is found in a three dimensional sense and then assumptions for plate formulations, e.g. plane stress or strain conditions, are applied.

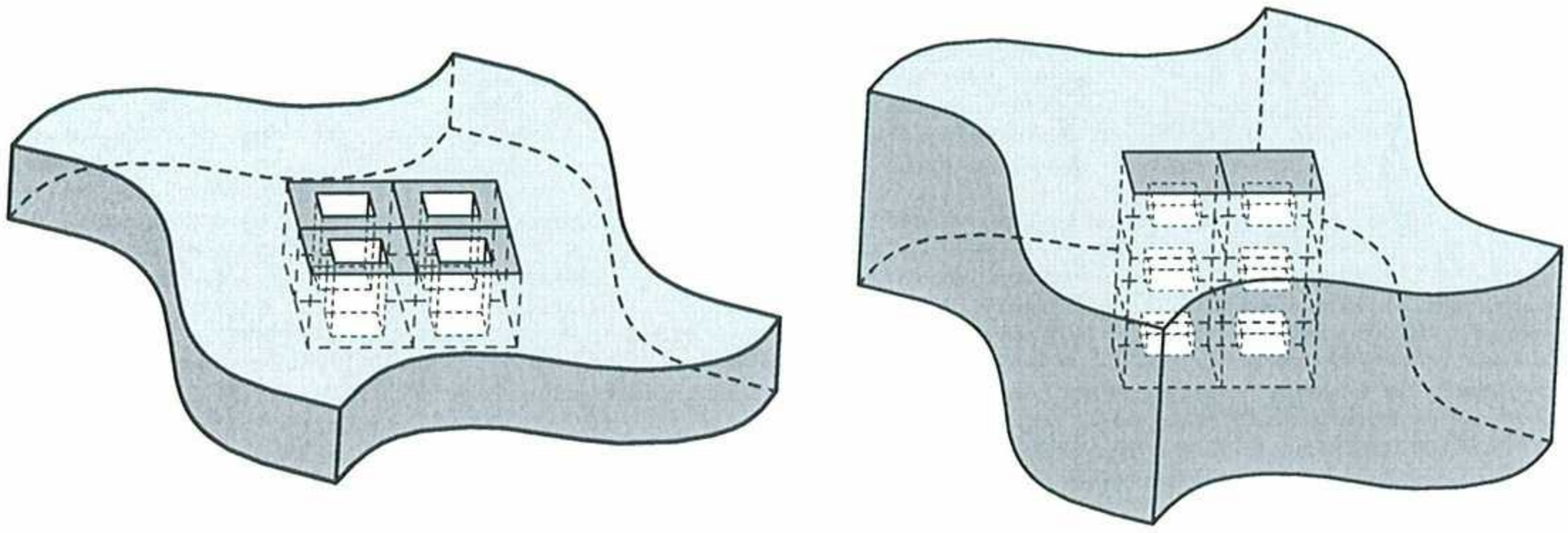

(a) (b)

Figure 1. The microstructure used for homogenization approaches, (a) a two dimensional model with through thickness hole for thin plate theory, (b) a three dimensional model with cubic hole inside a cube for thick plate theory.

To understand the differences of the models, the reader may note that for thin plates, shear deformations along z direction, γ_{xz} and γ_{yz}, are negligible and thus the 2-D model is well suited. However, for thick plates in which aforementioned shear deformations are not negligible, the 2-D model does not suffice to describe all properties of the real problem. In this latter case, the behavior of the cell, Figure 1-a, for shear stresses along z direction is different from that for shear stresses along x or y directions. In other words the 2-D model represents a "transversely orthotropic" material. Thus to account for shear deformation in thick plates with the 2-D model of Figure 1-a, a separate homogenization procedure is needed for calculation of the equivalent material constant for shear deformation.

For both models we define an equivalent density parameter as

$$\rho = \frac{V_{solid}}{V_{cell}} \tag{21}$$

and evaluate the material constants in terms of it. In above V_{solid} denotes the volume of the part filled with the material and V_{cell} represents the total volume of the cell. In that case M in (18) represents fraction of volume occupied by the material over the whole domain.

The matrix of the material constants is then evaluated as

$$\mathbf{d}_{\text{hom.}} = \begin{bmatrix} d_1 & d_2 & 0 \\ d_2 & d_1 & 0 \\ 0 & 0 & d_3 \end{bmatrix} \tag{22}$$

in which d_1, d_2 and d_3 are material constants and must satisfy the relations given in (10) if the homogenized material is to play the role of a real one, as we have assumed in this report (note that just two constants are needed for defining properties of a real homogenous-isotropic material). To this end, for the 2-D model, we first consider plane stress conditions, as usually assumed for plates, and apply a uniform constant strain along one of the main axes and calculate the average stresses at the faces of the cell representing the model of the microstructure. For the 3-D model, we first find material constants for a homogenized cube and then apply the plane stress conditions to the result. Finite element is employed for such computations. The procedure is straight forward and may be found in many papers (see Hassani and Hinton (1998) for instance). Having found the matrix of material constants as (22), the material modulus for plate problems can be obtained by suitable integration through thickness of the

plate. The corresponding modulus suitable for plate formulation is then evaluated as (9) when $\mathbf{d}$ is replaced with $\mathbf{d}_{\text{hom.}}$.

Variation of the elements of $\mathbf{d}$, in terms of the density defined in (21), is determined through evaluation of the elements at 100 data points of ρ. A curve fitting procedure is then employed for smoothing the discrete values. The curves are then used for calculation of the sensitivity values.

Design variables for laminated plates

In this type of problems, generally, ply angles of the fibers and the layout of the lamina are optimized. However, in this report, as discussed earlier, the laminae are assumed to consist of homogeneous-isotropic materials rather than orthotropic fibers. The optimal layout of the laminae, playing the role of stiffeners, may be determined either by the SIMP method (see for example Lee *et al* (2000) or Stegmann and Lund (2005)) or homogenization method (see for example Tenek and Hagiwara (1993)). In this report we shall employ the SIMP method. Thus the Young's modulus of the stiffeners (the second material in relation (17)), is expressed as a power law form

$$\mathbf{d}_2 = E_0\,\rho^m \begin{bmatrix} d_{11}^2 & d_{12}^2 & 0 \\ d_{21}^2 & d_{22}^2 & 0 \\ 0 & 0 & d_{33}^2 \end{bmatrix} \tag{23}$$

and is used in relation (17).

3.2 Mesh dependency, convergence problems and appearance of checkerboard patterns

A brief survey in the literature of topology optimization shows that occasionally the procedure suffers from the lack of convergence with respect to mesh refinement. Such an effect is seen in two/three dimensional problems especially when artificial materials are used. Several remedies have so far been proposed by many researchers. The reader may consult the review paper by Sigmund and Petersson (1998) and references therein. The effect stems from the fact that the problem is usually solved in a discrete manner with jumps in the DV while its solution is, in nature, continuous and smooth but may have sharp oscillation within infinitesimal lengths. To overcome such a difficulty an appropriate length scale, for controlling the variation of the DV, should be explicitly/implicitly defined in the solution. For plate problems, the effect turns out to be worse since these problems are degenerated from the three dimensional counterparts with some hypothesis. As mentioned earlier, this effect is much pronounced when artificial materials are used and this leads to ill-posed problems. Such an ill-posed-ness makes additional side effects, such as lack of convergence in the solution process (for example in mathematical programming approaches). This may happen even in one step of the optimization procedure, letting alone the convergence with respect to mesh refinement.

The problem of obtaining a checkerboard pattern is another effect usually seen in topology optimization. This effect is due to existence of an unrealistic solution to the discretized problem which represents an over-stiff structure.

The effects mentioned above are well known especially in the realm of two/three dimensional topology optimization. The remedies may in brief be classified as the following:

- *Restriction methods*: To alleviate the problem of mesh dependency, it is common to define some permissible lengths as bounds for variation of DV. For example in two dimensional problems the perimeter of the voids appearing in the optimization process may be restricted to be less than a specified value. By doing so another difficulty confronted is the problem of predefining suitable values for the bounds. The approach has mathematical bases and the reader may consult the paper by Haber et al 1996 or Petersson (1999).

Several other techniques are available for obtaining checkerboard free designs. A good summary may

be found in the monograph by Bendsøe and Sigmund (2003) and the references therein.

One important restriction method which seems to be relevant to the present study is using an upper bound for the norm of the gradients of the DV, i.e.

$$\left|\nabla\gamma\right| \le C \tag{24}$$

In above ∇ is the gradient operator, $\left|.\right|$ is an Euclidian norm and C is an appropriate upper bound value. Such restriction has been introduced by Niordson (1983) and used by Petersson and Sigmund (1998) in a point wise manner for two dimensional problems. It has been shown that the solution exists when $\left|\nabla\gamma\right| \le \frac{1}{3h}$ with h being the size of the square plate element. The method seems to be successful but the main problem is the time consumed for the application of the point-wise restrictions. Similar idea lies in the works in which nodal DV (as densities) are used (see Jog and Haber (1996) or the recent paper by Matsui and Terada (2004), for instance). The basic feature of such an approach is using continuous DV field while simultaneously controlling the gradient values by choosing appropriate value for allowable nodal values. In the studies mentioned, the nodes used for DV are the same as the ones used in the finite element analyses.

- *Filters:* A heuristic approach, which nowadays is widely accepted, is using a weighted averaging technique for DV and their gradients. It appears that the approach was first suggested by Sigmund (1994). Although the mathematical proof does not exist, the results of optimization are robust as experienced by many researchers (see Sigmund and Petersson (1998) and Bourdin (2001) for 2-D problems or Pedersen (2001) for plates). In this report we shall use the method in order to make comparison between the different approaches.

The filter has been proposed in two forms. The DV are averaged in a weighted form as

$$\hat{\gamma}_k = \frac{1}{\sum_{i=1}^{N} H\left(\overline{r}_{i-k}\right)\overline{r}_{i-k}} \sum_{i=1}^{N} H\left(\overline{r}_{i-k}\right)\overline{r}_{i-k}\,\gamma_i \tag{25-a}$$

$$\overline{r}_{i-k} = r_0 - r_{i-k} \tag{25-b}$$

In above N is the number of DV, r_{i-k} is the radial distance between spatial points allocated for variables k and i (e.g. the nodes or the center of the elements) and r_0 is the radius of the filter support defined by the user. Also H denotes the Heaviside function. A similar filter has been suggested for the sensitivity values

$$\hat{f}_{,\gamma_k} = \frac{1}{\gamma_k \sum_{i=1}^{N} H\left(\overline{r}_{i-k}\right)\overline{r}_{i-k}} \sum_{i=1}^{N} H\left(\overline{r}_{i-k}\right)\overline{r}_{i-k}\,\gamma_i f_{,\gamma_i} \tag{26}$$

Application of the filters to two dimensional problems results in a set of convergent, mesh independent results as shown by Sigmund and Petersson (1998) and Bourdin (2001). However, for plate problems the filter on the design variables seems to be not effective (see Pedersen (2001)).

- *Continuation methods*

Some of the techniques mentioned earlier may be used in a series of solutions while the specified parameters are gradually altered until a reasonable convergence is achieved. For instance the perimeter restriction may be applied gradually or even the power of density in the SIMP method can be altered from a small to a large value in a series of solutions. Another example is the use of filter in a sequential manner, i.e. step by step reducing the support area (see Sigmund and Petersson (1998)). However,

combination of the methods, e.g. using continuation on filters and on the power in SIMP, has not been recommended.

One important problem in using continuation methods is choosing the rate of changes in the parameters. This sometimes affects the convergence of the procedure as will be seen in the numerical examples. However, in the new continuation method proposed in the next section this is performed in a more systematic manner.

3.3 Node-based Design with Enhancive Resolution (NDER)

In this section we present a new continuation method based on continuous DV field. As we saw earlier in this report the idea of using nodal based DV interpolated with simple Lagrangian shape function has been examined by a number of scientists while some sort of instabilities has also been experienced. Obviously one remedy for such instabilities is using filters. However, as we shall present later, the rate of changing the influence area of the filter affects the solution. The remedy that we propose in this report is using different meshes for DV and the finite element solution.

Let $\mathcal{M}_{des.}$ denote the mesh used for DV. The elements in such a mesh are of Lagrangian type since the DV are just necessary to be interpolated without need for higher order continuity. Also let $\mathcal{M}_{anal.}$ denote the mesh used for finite element analysis. The elements in such a mesh are either of Lagrangian or Hermitian type depending on the formulation used for the solution, i.e. Mindlin or Kirchhoff type. If $h_{des.}$ and $h_{anal.}$ represent the elements size in $\mathcal{M}_{des.}$ and $\mathcal{M}_{anal.}$, respectively, then the procedure starts with element sizes so that

$$h_{des.} >> h_{anal.} \tag{27}$$

Note also that we are using square elements in this report. Although we can construct two different mesh sizes, here we assume that the ratio of $h_{des.}/h_{anal.}$ is a natural number i.e.

$$h_{des} = n\, h_{anal.},\ n \in \mathbb{N} \tag{28}$$

During the procedure n is sequentially reduced, so that $n \to 1$, while the mesh of finite element solution is maintained unchanged. The optimization procedure stops when convergence is obtained on mesh sizes with $n = 1$, i.e. when the two meshes are similar. Schematic presentation of the method is illustrated in Figure 2-a-c.

The following features are immediately recognized for the proposed method:

- When $n > 1$ the whole procedure of the interpolation of DV may be interpreted as a sort of averaging scheme. This resembles to the use of filters as Equation (25), though not quite similar. Also reducing the mesh size $\mathcal{M}_{des.}$ resembles the continuation method used for the filtering scheme. However choosing the rate of size reduction is straightforward, compared to that of filtering.

- During the optimization process the slope of the DV is restricted to a maximum value as $(\gamma_{\max} - \gamma_{\min})/(n\, h_{anal.})$. Note that DV values are always positive. It can be seen that when $n \to 1$ a continuation method is formed for maximum slope. The reader notes that the procedure may stop when $n \geq 1$ depending on the maximum allowable slope.

It is interesting to note that the procedure may be continued further so that

$$h_{des} = \frac{1}{m} h_{anal.},\ m \in \mathbb{N} \tag{29}$$

This means that one can use a DV mesh finer than the mesh used for the finite element solution. In doing so, two difficulties may be confronted.

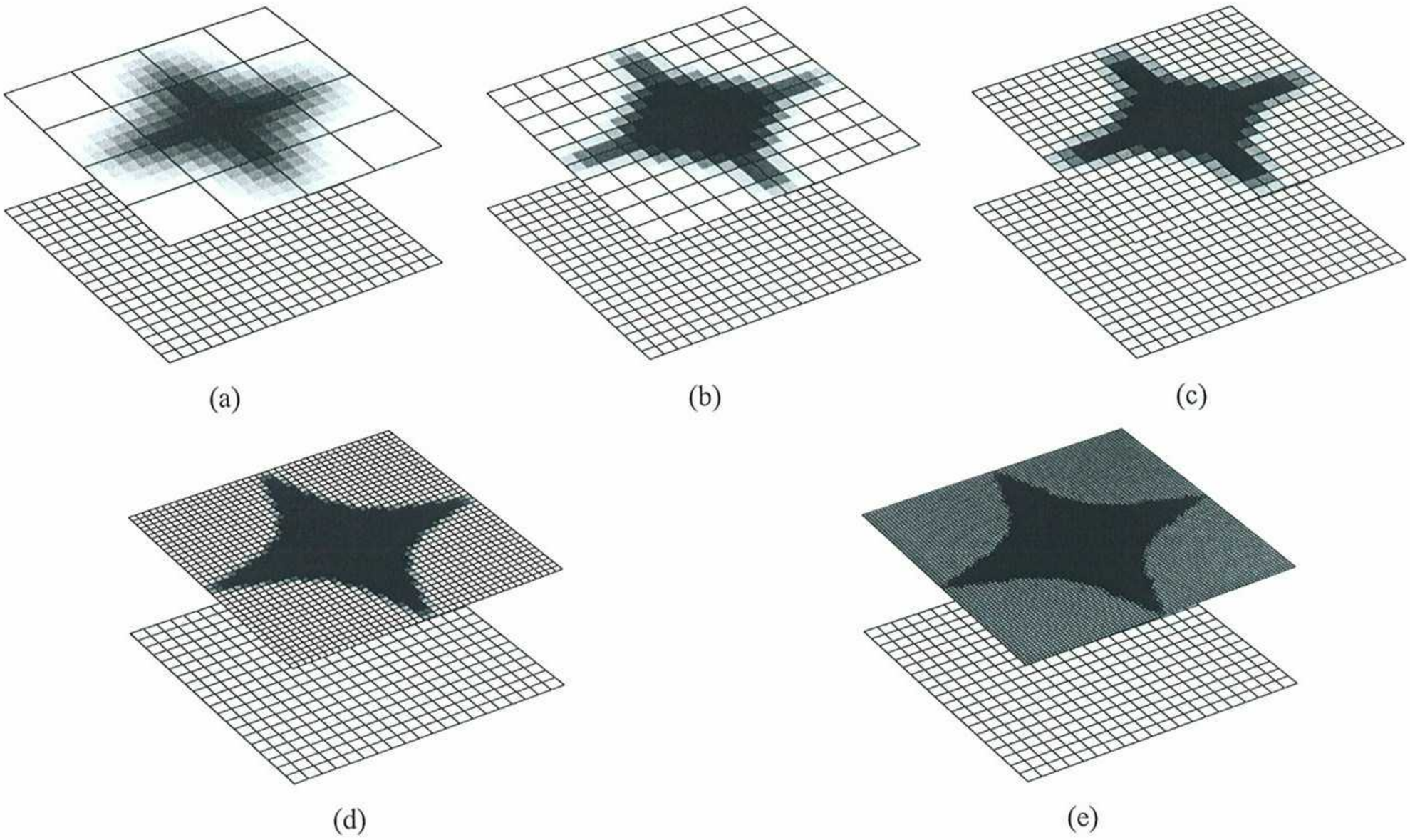

Figure 2. Schematic presentation of the sequential mesh refinement for design variables in NDER. In each pair the lower meshes represent the mesh used for finite element analysis and the upper one represent the mesh used for the design variables; in (a), (b) and (c) the design variable meshes are coarser than the finite element mesh; in (d) and (e) the design variable meshes are finer than the finite element mesh.

First one is the problem of non-uniqueness of the solution as discussed earlier. Our experience shows that once convergence is obtained on meshes with $n=1$, further refinements as $m>1$ leads to a sort of divergence in the solution. We shall propose a suitable treatment for this effect.

Second one is the order of integration needed for sharp variation of DV within an element. However for plate problems, this depends on the formulation used for the FE solution especially when Mindlin-Reissner type is used. A special low order integration scheme is usually needed for modeling the shear effects while the variation of the DV necessitates high order integration rule. Such a difficulty is not seen for formulation using Kirchhoff hypothesis. This may be regarded as an advantage of using Kirchhoff hypothesis in topology optimization of plates.

As a treatment of the first difficulty mentioned above, one can employ additional restraining approach for the optimization problem. Having found convergent results with $n=1$, on $\mathcal{M}_{des.}$ the nodes with minimum and maximum values for DV, i.e. $\overline{\gamma}=\gamma_{\min}$ and $\overline{\gamma}=\gamma_{\max}$ with the "bar" sign representing nodal value, are restrained against further changes when the procedure is to be continued for further refinement i.e. for $m>1$.

Such a restriction on the DV may raise a discussion on the possibility of the so called "rebirth of the node" similar to comments for evolutionary optimization schemes Xie and Steven (1993) made by some scientists (see Rozvany (2001)). However we note that obtaining convergent results on the meshes with $n=1$ means that the solution is very close to optimal one and thus by refining the mesh of DV we just intend to obtain topology with smoother edges and possibly with more details. Nevertheless, since the rebirth of the nodes may happen where the gradient of the DV is non-zero, we restrain all nodes of the elements in which the gradient vanishes. That means instead of performing a search on the nodes the search is performed on the elements.

In mesh refinement the integer number m should not be very large. Our experience shows that $m \leq 4$ gives reasonable results. Schematic presentation of the refinement is shown in Figure 2-d-e.

It is clear that changing the DV mesh, $\mathcal{M}_{des.}$, needs a suitable transfer operator to calculate nodal values of the new mesh. This means that

$$\overline{\gamma}_{new} = \mathbf{T}\left(\overline{\gamma}_{old}\right) \tag{30}$$

where $\overline{\gamma}$ represents vector of nodal DV used with subscript "old" and "new" to denote nodal values on old and new meshes in two consecutive refinements. Also $\mathbf{T}$ is a transfer operator shown in a matrix notation. When transferring information from old mesh to the new one, part of the information may be lost when new interpolation is performed on the new mesh. The effect is somewhat similar to what happens in adaptive procedures in nonlinear problems in solid mechanics (see Boroomand and Zienkiewicz (1999) and Peric *et al* (1996)). This probably becomes more serious when two unstructured meshes are used. To reduce the effect one may employ a direct Gauss point to Gauss point scheme as the one introduced in, e.g. see Boroomand and Zienkiewicz (1999), for adaptive nonlinear problems. When the design and analysis meshes consist of square elements such that (28) holds, the effect of information loss becomes immaterial since one can sometimes select the new element size so that not only (28) holds but also similar expression as $h_{des.}^{old} = k\, h_{des.}^{new}$ $(k \in \mathbb{N})$ exists between the two consecutive meshes of DV. However, even when such selection is not possible, in the case that a mathematical programming is used, the loss of information again becomes immaterial since the optimization procedure may start from the points outside the feasible domain. In that case the algorithm should be robust enough to find the feasible domain.

In summary the procedure of NDER is as follows

1- Construct a mesh for finite element analysis. Here we focus on meshes with square elements with edge size $h_{anal.}$.

2- Choose a series of meshes for design variables such that $h_{des} = n\, h_{anal.}$ with $n \in \mathbb{N}$. For instance if the finite element mesh, $\mathcal{M}_{anal.}$, consists of 20×20 elements we can choose a series of meshes, $\mathcal{M}_{des.}$, with 4×4, 5×5, 10×10 and 20×20 elements. If the elements used for finite element solution are so that they can easily model the variation of the design variables, we may further choose some meshes with $h_{des} = h_{anal.}/m$ with $m \in \mathbb{N}$. For example for $\mathcal{M}_{anal.}$ with 20×20 elements we may further choose $\mathcal{M}_{des.}$ with 40×40 or 80×80 elements.

3- Start from the coarse mesh of $\mathcal{M}_{des.}$ and the finite element mesh $\mathcal{M}_{anal.}$ and perform the optimization procedure until the required convergent criteria are met. The procedure of finite element solution considering variation of the DV with different mesh as $\mathcal{M}_{des.}$ combined with the optimization procedure which includes a consistent sensitivity analysis is described in the forthcoming sections.

4- Consider the next mesh of $\mathcal{M}_{des.}$, e.g. mesh number $i+1$, and find the position of the new nodes inside the previous mesh. Interpolate the nodal values of the old mesh to the new ones.

5- Perform the optimization procedure using the $\mathcal{M}_{anal.}$ and the new $\mathcal{M}_{des.}^{i+1}$ and continue it until the convergent criteria are met again.

6- Repeat from stage 4 until convergence is obtained on the final mesh of DV which is similar to the mesh of finite element solution. Stop the optimization procedure if no further fine mesh is to be used.

7- If finer meshes are to be used, i.e. when $m > 1$, again find the position of the new nodes inside the previous mesh. Interpolate the nodal values of the old mesh to the new one.

8- Perform a search over all elements of the new mesh and calculate the absolute value of the gradient of the DV at the center of the element. If the absolute value is zero or less than a specified value, nominate all nodes of the element for restraining against further changes. At the end of such a search all nodes nominated for restraining are listed.

9- Modify the first part of the side constraint of (18) as

$$\int_{A-A_r^1-A_r^2} \gamma dA \le M - \int_{A_r^1} \gamma_{\max} dA - \int_{A_r^2} \gamma_{\min} dA \tag{31}$$

In which A_r^1 and A_r^2 denote the parts of plate area on which change of design variable is not permitted and are pertaining to maximum and minimum values of the design variable, respectively.

10- Perform the optimization procedure with remaining nodal DV, using the $\mathcal{M}_{anal.}$ and the new $\mathcal{M}_{des.}$, and continue it until the convergent criteria are met again.

11- Repeat from step 7 if finer mesh is to be employed.

The reader may notice that the proposed procedure can be used in more general way, i.e. use of the continuation method in an adaptive manner. This means that a series of structured/unstructured meshes can be used while considering an appropriate criterion for refinement. Therefore as discussed earlier a suitable transfer operator is needed so that the constraints are not violated severely. Such a procedure needs more elaboration on choosing various $\mathcal{M}_{des.}$ and can be the issue of a separate report. Here we aim at examining the robustness and convergence of the optimization problem on structured mesh with regular square elements.

3.4 Finite Element Analysis combined with NDER

In this section we overview the finite element analysis of plates while considering that the DV are interpolated on a separate mesh.

Finite element analysis of plates starts from discretization of the domain along with the use of suitable interpolation functions for the main unknowns. The formulation is straight forward and can be found in many finite element text books, e.g. Zienkiewicz and Taylor (2000). A summary of the formulations for both Kirchhoff and Mindlin-Reissner hypothesis is given in Table 1. In the part pertaining to Kirchhoff formulation $\mathbf{N}^{u}_{0-\mathcal{M}_{anal.}}$ denotes a set of Lagrangian shape functions (hat functions) for in-plane displacements and $\mathbf{N}^{w}_{1-\mathcal{M}_{anal.}}$ represents a set of appropriate shape functions producing C^1 continuity (e.g. Hermit type) for the deflection field. For the part pertaining to Mindlin-Reissner formulation $\mathbf{N}^{u}_{0-\mathcal{M}_{anal.}}$, $\mathbf{N}^{w}_{0-\mathcal{M}_{anal.}}$ and $\mathbf{N}^{\theta}_{0-\mathcal{M}_{anal.}}$ denote sets of Lagrangian shape functions for in-plane displacements, deflection field and rotation field, respectively.

As mentioned earlier we shall use continuous fields of the DV. Therefore we interpolated the values from nodal quantities as

$$t = \mathbf{N}^{t}_{\mathcal{M}_{des.}} \overline{\mathbf{t}} \quad \text{or} \quad \rho = \mathbf{N}^{\rho}_{\mathcal{M}_{des.}} \overline{\boldsymbol{\rho}} \tag{32}$$

Here $\mathbf{N}_{\mathcal{M}_{des.}}$ denotes hat-shape functions over the DV mesh and the superscripts in (32) refer to the type of the DV chosen. The shape functions are obviously of Lagrangian type.

The elements used

When using Kirchhoff hypothesis, bilinear shape-functions are used for in-plane displacements, and a set of shape-functions introduced by Zienkiewicz and Cheung (1964) are used for out of plane deflection.

When using Mindlin-Reissner hypothesis, nine node elements are used for in-plane displacements, and for out of plane deflections we follow the formulation and shape-functions introduced by Hughes and Cohen (1978) called Heterosis elements.

Table 1. Summary of finite element formulations and sensitivity relations for plate modeled with Kirchhoff and Mindlin-Reissner hypothesis

	Kirchhoff hypothesis	Mindlin-Reissner hypothesis
Interpolation	$\mathbf{u} \simeq \hat{\mathbf{u}} = \begin{bmatrix} \hat{u} & \hat{v} \end{bmatrix}^T = \mathbf{N}^u_{0-\mathcal{M}_{anal.}} \bar{\mathbf{u}}$ $w \simeq \hat{w} = \mathbf{N}^w_{1-\mathcal{M}_{anal.}} \bar{\mathbf{w}}$ $\bar{\mathbf{w}}$ includes nodal deflections and rotations $\bar{\mathbf{U}} = \bar{\mathbf{u}} \cup \bar{\mathbf{w}}$	$\mathbf{u} \simeq \hat{\mathbf{u}} = \begin{bmatrix} \hat{u} & \hat{v} \end{bmatrix}^T = \mathbf{N}^u_{0-\mathcal{M}_{anal.}} \bar{\mathbf{u}}$ $w \simeq \hat{w} = \mathbf{N}^w_{0-\mathcal{M}_{anal.}} \bar{\mathbf{w}}$ $\bar{\mathbf{w}}$ includes nodal deflections $\boldsymbol{\theta} \simeq \hat{\boldsymbol{\theta}} = \mathbf{N}^\theta_{0-\mathcal{M}_{anal.}} \bar{\boldsymbol{\theta}}$ $\bar{\mathbf{U}} = \bar{\mathbf{u}} \cup \bar{\mathbf{w}} \cup \bar{\boldsymbol{\theta}}$
Residuals	$\Psi = \int_A \left(\mathbf{B}^{pb}\right)^T \mathbf{D}^{pb} \tilde{\mathbf{B}}^{pb} \bar{\mathbf{U}} dA - \mathbf{F} = \mathbf{0}$ $\mathbf{B}^{pb}$ is a matrix relating the variation of the strains to the variation of the nodal displacements/rotations as $\delta \mathbf{E}^{pb} = \mathbf{B}^{pb} \delta \bar{\mathbf{U}}$ $\tilde{\mathbf{B}}^{pb}$ is a matrix relating the strains to the nodal displacements/rotations as $\mathbf{E}^{pb} = \tilde{\mathbf{B}}^{pb} \bar{\mathbf{U}}$	$\Psi = \int_A \left(\mathbf{B}^{psb}\right)^T \mathbf{D}^{psb} \tilde{\mathbf{B}}^{psb} \bar{\mathbf{U}} dA - \mathbf{F} = \mathbf{0}$ $\mathbf{B}^{psb}$ is a matrix relating the variation of the strains to the variation of the nodal displacements/rotations as $\delta \mathbf{E}^{psb} = \mathbf{B}^{psb} \delta \bar{\mathbf{U}}$ $\tilde{\mathbf{B}}^{psb}$ is a matrix relating the strains to the nodal displacements/rotations as $\mathbf{E}^{psb} = \tilde{\mathbf{B}}^{psb} \bar{\mathbf{U}}$
Matrix of Material constant	$\mathbf{D}^{pb} = \begin{bmatrix} \mathbf{D}^p & \mathbf{0} \\ \mathbf{0} & \mathbf{D}^b \end{bmatrix}$	$\mathbf{D}^{psb} = \begin{bmatrix} \mathbf{D}^p & \mathbf{0} & \mathbf{0} \\ \mathbf{0} & \mathbf{D}^s & \mathbf{0} \\ \mathbf{0} & \mathbf{0} & \mathbf{D}^b \end{bmatrix}$
Split of the loads	$\mathbf{F}^l = \sum_{j=1}^{l} \Delta \mathbf{F}^j \ , \ \bar{\mathbf{U}}^l = \bar{\mathbf{U}}^{l-1} + \Delta \bar{\mathbf{U}}^l$	$\mathbf{F}^l = \sum_{j=1}^{l} \Delta \mathbf{F}^j \ , \ \bar{\mathbf{U}}^l = \bar{\mathbf{U}}^{l-1} + \Delta \bar{\mathbf{U}}^l$
Linearization	$i = 1, 2, \ldots$ $\Psi_i \approx \Psi_{i-1} + \left(\frac{\partial \Psi}{\partial \bar{\mathbf{U}}}\right)_{i-1} \delta \bar{\mathbf{U}}_i = \mathbf{0}$ $\delta \bar{\mathbf{U}}^l_i = -\left[\mathbf{K}_{T_{i-1}}\right]^{-1} \Psi^l_{i-1}$ $\Delta \bar{\mathbf{U}}^l = \sum_i \delta \bar{\mathbf{U}}^l_i$	$i = 1, 2, \ldots$ $\Psi_i \approx \Psi_{i-1} + \left(\frac{\partial \Psi}{\partial \bar{\mathbf{U}}}\right)_{i-1} \delta \bar{\mathbf{U}}_i = \mathbf{0}$ $\delta \bar{\mathbf{U}}^l_i = -\left[\mathbf{K}_{T_{i-1}}\right]^{-1} \Psi^l_{i-1}$ $\Delta \bar{\mathbf{U}}^l = \sum_i \delta \bar{\mathbf{U}}^l_i$
Sensitivity of the residuals	$\frac{\partial \Psi}{\partial \bar{\gamma}_k} = \int_A \left(\mathbf{B}^{pb}\right)^T \frac{\partial \mathbf{D}^{pb}}{\partial \bar{\gamma}_k} \tilde{\mathbf{B}}^{pb} \bar{\mathbf{U}} dA$	$\frac{\partial \Psi}{\partial \bar{\gamma}_k} = \int_A \left(\mathbf{B}^{psb}\right)^T \frac{\partial \mathbf{D}^{psb}}{\partial \bar{\gamma}_k} \tilde{\mathbf{B}}^{psb} \bar{\mathbf{U}} dA$
Sensitivity of the material constants	$\frac{\partial \mathbf{D}^{pb}}{\partial \bar{\gamma}_k} = \begin{bmatrix} \frac{\partial \mathbf{D}^p}{\partial \bar{\gamma}_k} & \mathbf{0} \\ \mathbf{0} & \frac{\partial \mathbf{D}^b}{\partial \bar{\gamma}_k} \end{bmatrix}$	$\frac{\partial \mathbf{D}^{psb}}{\partial \bar{\gamma}_k} = \begin{bmatrix} \frac{\partial \mathbf{D}^p}{\partial \bar{\gamma}_k} & \mathbf{0} & \mathbf{0} \\ \mathbf{0} & \frac{\partial \mathbf{D}^s}{\partial \bar{\gamma}_k} & \mathbf{0} \\ \mathbf{0} & \mathbf{0} & \frac{\partial \mathbf{D}^b}{\partial \bar{\gamma}_k} \end{bmatrix}$

3.5 The objective function

In this report we shall use complimentary work as the objective function

$$f = \frac{1}{2}\left[\Delta \mathbf{F}_0^T \bar{\mathbf{U}}_0 + \sum_{j=1}^{n-1} \left(\Delta \mathbf{F}_{j-1}^T + \Delta \mathbf{F}_j^T \right) \bar{\mathbf{U}}_j + \Delta \mathbf{F}_n^T \bar{\mathbf{U}}_n \right] \tag{33}$$

In above $\Delta \mathbf{F}$ represents the load increment and $\bar{\mathbf{U}}$ denotes total nodal values, at the end of the load steps, obtained after convergence of the non-linear finite element solution.

3.6 Sensitivity analyses

A mathematical programming approach is employed for optimization in this report. Therefore a sensitivity analysis is performed through the well-known adjoint method.

The adjoint method

For optimization procedures in which the objective function are dependent on the history of the displacements, like the one we use in this report, the sensitivity analyses can be performed through a solution of suitable adjoint problem.

When the residuals at the end of each load step become sufficiently small the objective function may be written as

$$f = f + \sum_{j=1}^{n} \boldsymbol{\lambda}_j^T \boldsymbol{\Psi}_j , \ \boldsymbol{\Psi}_j \simeq \mathbf{0} \tag{34}$$

where $\boldsymbol{\lambda}_j$ are vectors of arbitrary multipliers to be defined. The procedure of computing the vectors of multipliers can be found in the literature. Here we just mention the final results

$$\boldsymbol{\lambda}_j = -\left[\mathbf{K}_T^j \right]^{-1} \frac{\partial f}{\partial \bar{\mathbf{U}}_j} \tag{35}$$

Where $\mathbf{K}_T^j$ is the tangent stiffness matrix evaluated at the end of the Newton-Raphson iteration. From (34) one can calculate the sensitivities as

$$\frac{\partial f}{\partial \gamma_k} = \sum_{j=1}^{n} \boldsymbol{\lambda}_j^T \frac{\partial \boldsymbol{\Psi}_j}{\partial \gamma_k} \tag{36}$$

In above γ_k is the kth element/nodal value of the DV in the associated mesh. Summary of the sensitivities of the residuals is given in Table 2.

The reader may notice that when element based design variables are used, the sensitivity values can be calculated at element level as usually performed in the literature. However, when nodal based DV are used, the sensitivity values should be evaluated as the assembly of contributions from elements connected to (or containing) the kth node in the mesh of the DV, i.e. on all elements in the main FE mesh in which the hat function $N_{\mathcal{M}_{des.}}^{\bar{\gamma}_k}$ is non-zero.

Thickness and density as the DV: Using thickness and density as the element/nodal based DV is straightforward and a summary of the formulations are given in Table 2. It may be noted that the orders of the DV, i.e. t and ρ, are not similar in different parts of the sensitivity expressions. This leads to different paths for attaining the optimal design.

Solid volume as the DV (in the homogenization approach): When solid volume is used as the DV (see relation (21) for equivalent density) utilizing nodal values implies that elements of $\mathbf{d}$ matrix vary inside

a generic plate element. This, however, contradicts with the assumptions usually made for homogenization of the perforated material (the reader may note that a sort of periodicity assumption is used to derive the relations for the homogenization, see Hassani and Hinton (1998) for instance).

Table 2. Summary of sensitivity relations for matrix of material constants when plate is modeled with Kirchhoff and Mindlin-Reissner hypothesis and different design variables are used.

	Element based variable on mesh $\mathcal{M}_{anal.}$	Nodal based variable on mesh $\mathcal{M}_{des.}$
Thickness as the design variable	$\frac{\partial \mathbf{D}^p}{\partial \overline{t}_k} = \mathbf{d}$ $\frac{\partial \mathbf{D}^b}{\partial \overline{t}_k} = \frac{\overline{t}_k^2}{4}\mathbf{d}$ $\frac{\partial \mathbf{D}^s}{\partial \overline{t}_k} = E\alpha d_{33}\mathbf{I}_{2\times 2}$	$\frac{\partial \mathbf{D}^p}{\partial \overline{t}_k} = N^{\overline{t}_k}_{\mathcal{M}_{des.}}\mathbf{d}$ $\frac{\partial \mathbf{D}^b}{\partial \overline{t}_k} = \frac{N^{\overline{t}_k}_{\mathcal{M}_{des.}} t^2}{4}\mathbf{d}$ $\frac{\partial \mathbf{D}^s}{\partial \overline{t}_k} = E\alpha N^{\overline{t}_k}_{\mathcal{M}_{des.}} d_{33}\mathbf{I}_{2\times 2}$
Density as the design variables	$\frac{\partial \mathbf{D}^p}{\partial \overline{\rho}_k} = m\overline{\rho}_k^{-1}\mathbf{d}$ $\frac{\partial \mathbf{D}^b}{\partial \overline{\rho}_k} = \frac{m\overline{\rho}_k^{-1}t^3}{12}\mathbf{d}$ $\frac{\partial \mathbf{D}^s}{\partial \overline{\rho}_k} = \left(\alpha m\,\overline{\rho}_k^{m-1}E_0 d_{33}t\right)\mathbf{I}_{2\times 2}$	$\frac{\partial \mathbf{D}^p}{\partial \overline{\rho}_k} = m\rho^{-1}N^{\overline{\rho}_k}_{\mathcal{M}_{des.}}\mathbf{d}$ $\frac{\partial \mathbf{D}^b}{\partial \overline{\rho}_k} = \frac{m\rho^{-1}t^3}{12}N^{\overline{\rho}_k}_{\mathcal{M}_{des.}}\mathbf{d}$ $\frac{\partial \mathbf{D}^s}{\partial \overline{\rho}_k} = \left(\alpha m\,\rho^{m-1}E_0 d_{33}t\right)N^{\overline{\rho}_k}_{\mathcal{M}_{des.}}\mathbf{I}_{2\times 2}$
Solid volume as the design variable in homogenization	$\frac{\partial \mathbf{D}^p}{\partial \overline{\rho}_k} = t\left(\frac{\partial}{\partial \overline{\rho}_k}\mathbf{d}\right)$ $\frac{\partial \mathbf{D}^b}{\partial \overline{\rho}_k} = \frac{t^3}{12}\left(\frac{\partial}{\partial \overline{\rho}_k}\mathbf{d}\right)$ $\frac{\partial \mathbf{D}^s}{\partial \overline{\rho}_k} = \left(\alpha E t\,\frac{\partial d_{33}}{\partial \overline{\rho}_k}\right)\mathbf{I}_{2\times 2}$	$\rho^C_{elem} = \left[\mathbf{N}^{\rho}_{\mathcal{M}_{des.}}\right]_{\xi=\overline{\xi},\eta=\overline{\eta}}\overline{\boldsymbol{\rho}}$ $\left[\frac{\partial \mathbf{D}^p}{\partial \overline{\rho}_k}\right]^C_{elem} = t\left[N^{\overline{\rho}_k}_{\mathcal{M}_{des.}}\left(\frac{\partial}{\partial \rho}\mathbf{d}\right)\right]_{\xi=\overline{\xi},\eta=\overline{\eta}}$ $\left[\frac{\partial \mathbf{D}^b}{\partial \overline{\rho}_k}\right]^C_{elem} = \frac{t^3}{12}\left[N^{\overline{\rho}_k}_{\mathcal{M}_{des.}}\left(\frac{\partial}{\partial \rho}\mathbf{d}\right)\right]_{\xi=\overline{\xi},\eta=\overline{\eta}}$ $\left[\frac{\partial \mathbf{D}^s}{\partial \overline{\rho}_k}\right]^C_{elem} = \left(\alpha E t\right)\left[\frac{\partial d_{33}}{\partial \rho}N^{\overline{\rho}_k}_{\mathcal{M}_{des.}}\right]_{\xi=\overline{\xi},\eta=\overline{\eta}}\mathbf{I}_{2\times 2}$
Density of the laminae representing the stiffeners in laminated plates	$\frac{\partial \mathbf{D}^p}{\partial \overline{\rho}_k} = 2t_s m\overline{\rho}_k^{-1}\mathbf{d}_2$ $\frac{\partial \mathbf{D}^b}{\partial \overline{\rho}_k} = \frac{m\,\overline{\rho}_k^{-1}\left[\left(h+2t_s\right)^3 - h^3\right]}{12}\mathbf{d}_2$	$\frac{\partial \mathbf{D}^p}{\partial \overline{\rho}_k} = 2t_s m\rho^{-1}N^{\overline{\rho}_k}_{\mathcal{M}_{des.}}\mathbf{d}_2$ $\frac{\partial \mathbf{D}^b}{\partial \overline{\rho}_k} = \frac{m\,\rho^{-1}\left[\left(h+2t_s\right)^3 - h^3\right]}{12}N^{\overline{\rho}_k}_{\mathcal{M}_{des.}}\mathbf{d}_2$

Therefore it seems logical to use a constant material property at a generic plate element. For this, we have just used the values at the center of the elements. Note that such central value for the density is still dependent on the nodal values of the mesh of the DV. Summary of the relations are given in Table 2. In the table superscript C is used to denote that the variable is taken as a constant over the element.

Also (ξ,η) is a pair of local coordinates at the element of the DV, and $\overline{\xi},\overline{\eta}$ are local coordinates of the center of the plate element in the design mesh.

In using the homogenization method, the sensitivity calculation requires derivatives of the homogenized-material properties. To this end a sensitivity analysis may be performed on finite element solution that pertains to the homogenization technique. However, for simplicity, we have used curves fitted to discrete values obtained from the homogenization process.

Density of the stiffeners as the DV: Sensitivity analysis for laminated plates is also straightforward and the summary is presented in Table 2. Note that in this case we have just used the SIMP method.

In order to include the effects of shear deformations, at least in its first order form, one needs to define a shear coefficient for Mindlin-Reissner formulation. Since such a coefficient is dependent on the stiffness ratio of the layers, it will be dependent on the DV (here the density). Therefore the sensitivity analyses will be complicated. By neglecting such a dependency one can alternatively use approximations similar to that used by Lee *et al* (2000) or Stegmann and Lund (2005). As we mentioned earlier we shall use a classical theory of laminates in this report. Therefore the relations for Mindlin-Reissner formulations are not given in Table 2.

3.7 Minimization procedure

The Method of Moving Asymptotes (MMA) introduced by Svanberg 1987 & 2002 is employed in this report for the minimization process. The algorithm has been proved to be effective for a wide range of large scale topology optimization problems. Here we avoid explaining the details of the algorithm but it is just mentioned that the method finds the optimal design variables in an iterative manner. In each iteration step an approximation of the objective is used by defining appropriate asymptotes. The iteration is assumed to reach to convergent results when variations of the constraints and the objective function are less than specified values. For comparison between the results of different approaches we shall monitor the convergence path obtained by MMA in the presented problems.

4. NUMERICAL RESULTS

In this section we present numerical results using NDER for some sample problems. For the sake of comparison, other results will also be given for approaches such as Element and Nodal Based optimization. By the Element Based approach we seek for topology defined by discontinuous DV with constant values over each element of the mesh used for the FE solution. By the Nodal Based approach, the topology is obtained via continuous field of DV defined by a set of linear shape functions and nodal values over a discretized domain similar to that used for the FE solution.

Wherever is needed we shall use filter, as Equation (25) in both approaches. However for using filters, in a continuation style, a tuning procedure is needed for defining the change rate in the influence area of the filter, i.e. area defined by r_0 in (25).

We have performed such a study on a series of linear rectangular plate problems. The results are applied to all other cases in linear and nonlinear problems. Our experience shows that the optimal change rate of r_0 is dependent on the finite element mesh size. This means that finer meshes usually need more steps for reduction of r_0. For example for a mesh of $NE\times NE$ square elements the number of steps for reduction of r_0 is approximately $NE/2$ (or $Int\left(NE/2\right)$ if NE is an even (or odd number). We have obtained the following heuristic formula for r_0 in i th step

$$r_0^i=\sqrt{2}\left(NE-2i+n_0\right)h,\ i=1,2,.....,NE/2 \tag{38}$$

where h is the element size and n_0 is an appropriate number for controlling minimum size of r_0. For

example if we require that the smallest influence area of the filter contain all surrounding nodes/elements of a node/element, then we choose $n_0 = 1$ (note that here NE is an even number). In order to obtain a mesh independent topology using two distinct meshes, with different numbers of elements for finite element analysis, NE, we adjust n_0 so that the minimum influence areas in the two cases become identical.

Obviously some other choices are still possible for the step sizes in reduction of r_0. We shall give some results on the effect of choosing different rates for reduction of r_0. Our experience also shows that the optimal rate is dependent on the magnitude of shear deformations.

Various DV, as described earlier, are used to obtain the results. The maximum and minimum of the DV, are as summarized in Table 3.

Table 3. Maximum and minimum of the design variables

DV	Min	Max
$\gamma = t$	0.001	3 (problem 1) 150 (problem 2)
$\gamma = \rho$ SIMP	0.001 ($\rho_{thresh} = 0.25$)	1.0
$\gamma = V_{solid} / V_{cell}$ Homogenization	0.001	1.0
$\gamma = \rho$ SIMP Laminated plate	0.0 ($\rho_{thresh} = 0.0$)	1.0
	the thicknesses of the top and bottom layers are taken as $t_s = t/4$	

Sample problem 1. A simply supported rectangular thin plate under a point load at the center is considered for topology optimization (see Figure 3-a). The aim is to obtain a plate-like perforated structure with minimum complimentary work. The structure is to be obtained on a square area with edge length of $L_x = L_y = 2\ m$ and maximum thickness of $t = 3mm$. The Young's modulus and the Poisson's ratio of the material are chosen as $E = 200\ GPa$ and $\nu = 1/3$. A point load of $80\,N$ is considered for linear analysis. For nonlinear analysis however we use a load of $800\ N$. The topology optimization is performed with 30% of the material. The problem is solved with Kirchhoff hypothesis.

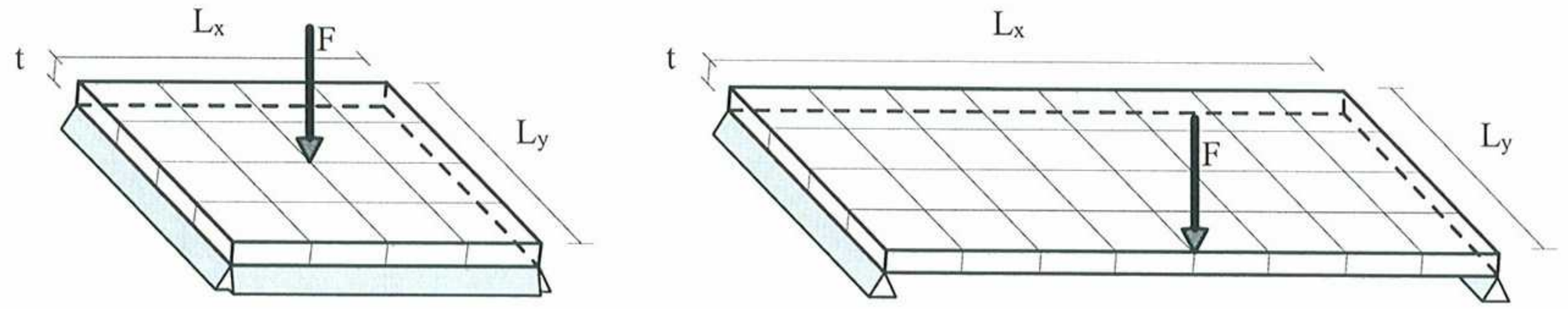

Figure 3. The geometry of the plates used for sample problems; (a) a square plate with simply supports at all four edges used for sample problems No.1 and 2, (b) a rectangular plate with three simply supports and one free edge for Sample problem No. 3.

For the first series of solutions the finite element mesh consists of 20×20 square elements. Hard simply supports are considered during finite element modeling. Due to symmetry of the domain a

quadrant of the mesh, i.e. an area with 10×10 elements, together with a set of appropriate boundary conditions at the axes of symmetry of the domain, is considered. The topologies obtained by different approaches and various choices of DV are listed in Figure 4. Performance of the three forms of approaches, namely the element based one using filter, the node based one with filter and the new one using NDER are examined.

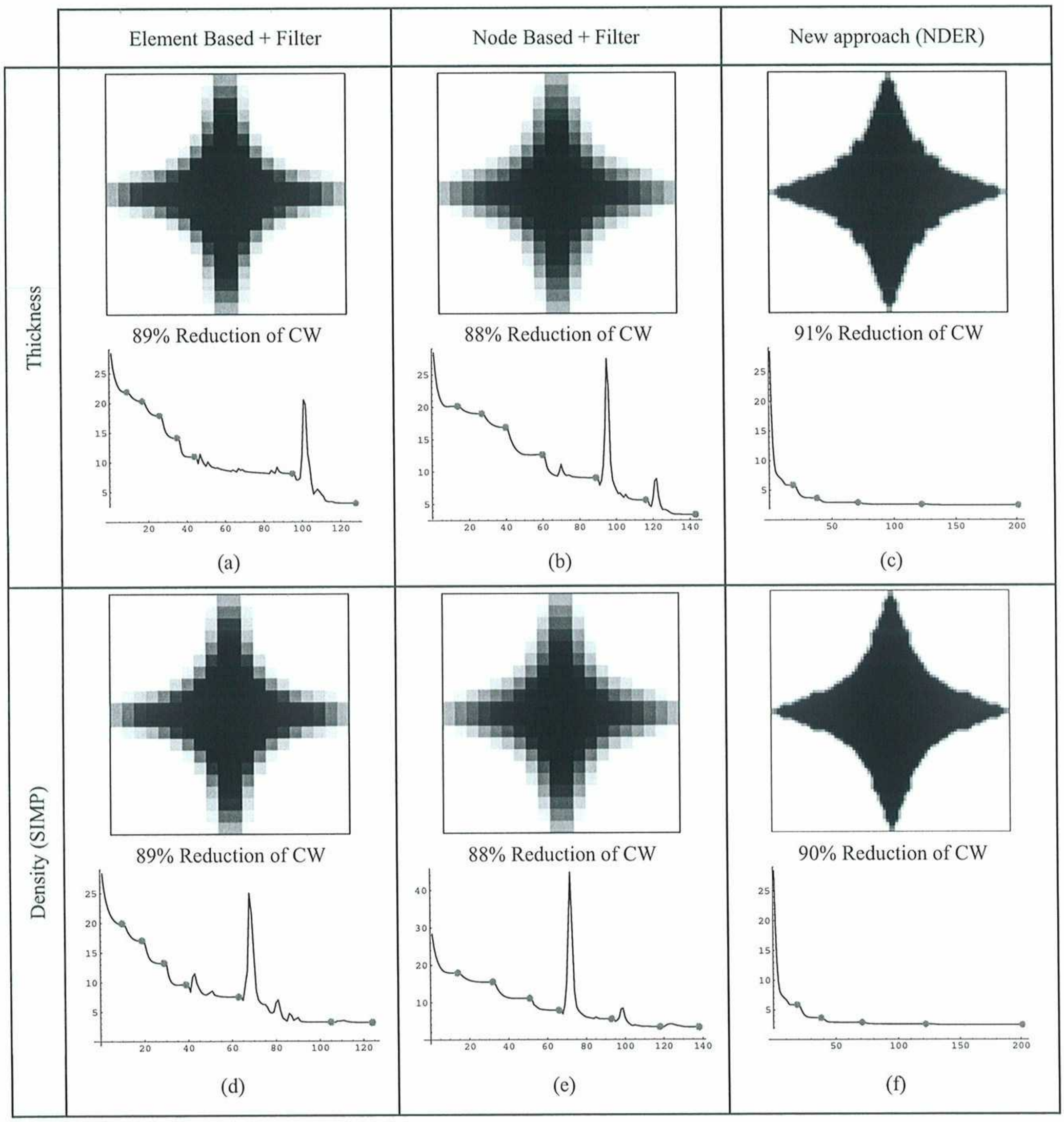

Figure 4. Topologies obtained by different approaches and various choices of design variables for sample problem No.1 when linear behavior is assumed. A mesh of 20×20 square elements is used for finite element solution. Topology and convergence plot for; (a) element based approach using filter and thickness as the design variables, (b) nodal based approach using filter and thickness as the design variables (c) NDER and thickness as the design variables, (d) element based approach using filter and density, in SIMP method, as the design variables, (e) nodal based approach using filter and density, in SIMP method, as the design variables, (f) NDER and density, in SIMP method, as the design variables,

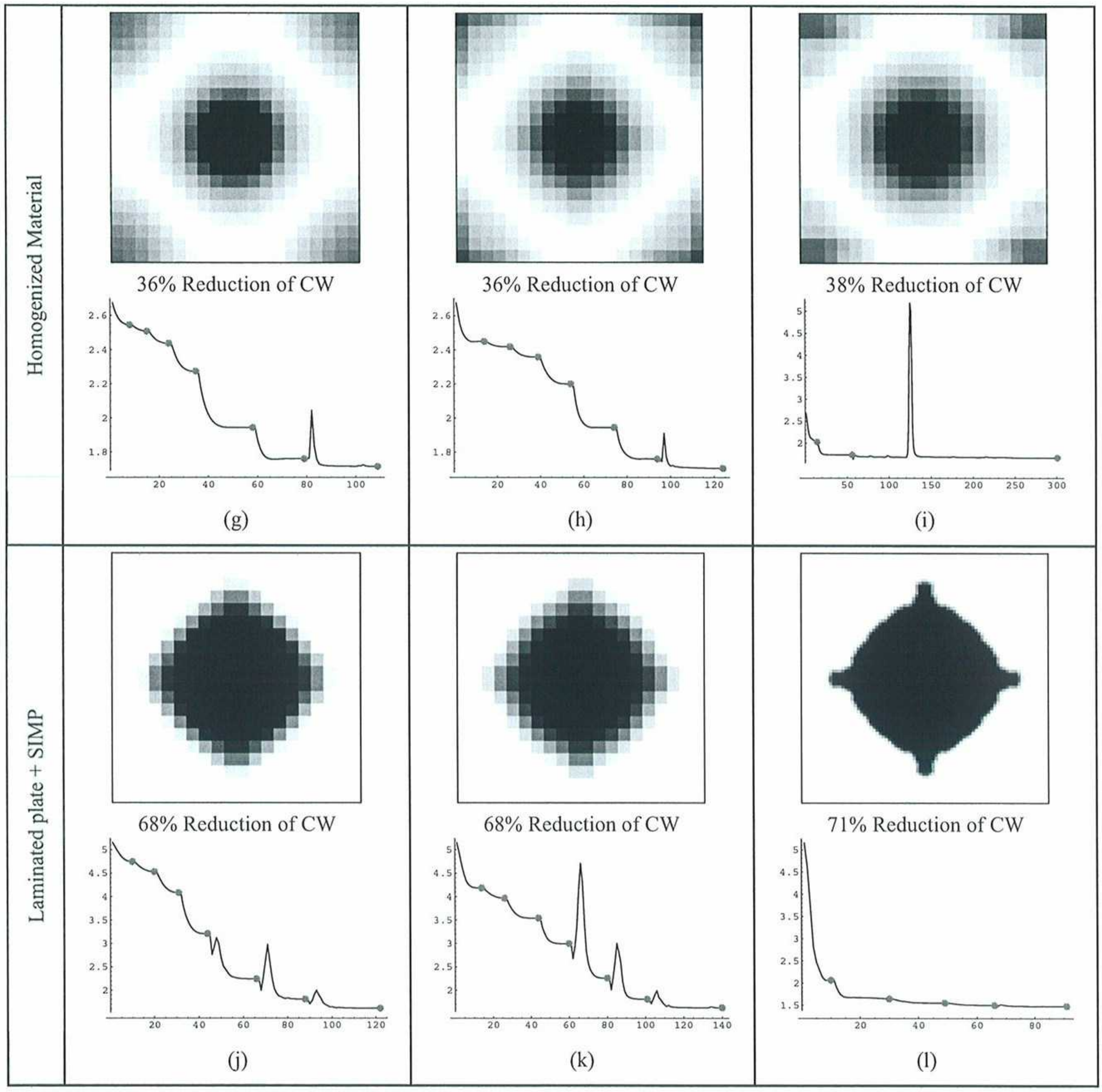

Figure 4. (continued) (g) element based approach using filter and the equivalent density, in homogenization method with Model No.1, as the design variables, (h) nodal based approach using filter and the equivalent density, in homogenization method with Model No.1, as the design variables (i) NDER and the equivalent density, in homogenization method with Model No.1, as the design variables, (j) element based approach using filter and density of the top and bottom layers, in SIMP method, as the design variables, (k) nodal based approach using filter and density of the top and bottom layers, in SIMP method, as the design variables (l) NDER and density of the top and bottom layers, in SIMP method, as the design variables.

For NDER method, meshes with 2×2, 5×5, 10×10, 20×20 and 40×40 elements are considered for the $\mathcal{M}_{des.}$ (the last two meshes are finer than the finite element mesh and are used for all methods except the homogenization one). The results, from application of the new method, are shown on the final mesh. Figures 4-a-f show that, when thickness and density play the role of the DV, the results are quite similar. As expected the topology obtained from NDER is very clear compared to those obtained from the other two approaches. The overall configurations of the topologies agree with the results obtained by Pedersen (2001).

The topologies obtained with homogenized material, Figures 4-g-I, are quite different from those obtained with thickness and density. For homogenization procedure Model No. 1 (see Figure 1-a) is employed.

Since no penalization is applied to the procedure some gray areas representing intermediate densities are seen in the topologies. Note also that in this approach the results of NDER are similar to those of the other two approaches. The reason lies in the fact that we did not use fine meshes in this case (recall the assumptions for homogenization and what earlier described for constant value for the design variable).

The results for laminated plate using SIMP method are also interesting, Figures 4-j-l. These are somewhat similar to those with homogenized material. Note that the figures are representative of topology of stiffeners since a layer of filler material is still remaining. The overall configuration of the topologies agree with the results obtained by Lee *et al* (2000).

Figures representing convergence of the solutions are given below the topologies. The horizontal axes demonstrate the number of steps used for optimization and the numbers on the vertical axes represent the values of the objective function (i.e. complimentary work). From the convergence figures it can easily be seen that the rate of convergence in NDER is much more than that of element and nodal based methods with filters. One exception is recognized in homogenization method in which an unusual spike is seen in the results of NDER but convergence has essentially been obtained before the spike (the spike is due to the change in $\mathcal{M}_{des.}$).

To examine the mesh dependency of the method, second series of the solutions are given in Figures 5. In NDER method we have used a 20×20 square element mesh for a quadrant of the domain for finite element solution, i.e. $\mathcal{M}_{anal.}$. A set of meshes with 4×4, 5×5, 10×10 and 20×20 elements are used for design variables, $\mathcal{M}_{des.}$. We have also used a finer mesh with 40×40 elements mesh but have not proceeded further in order to obtain results comparable with those of the previous set in Figure 4. The topologies obtained are similar to those of Figure 4. The same conclusions as discussed earlier for Figure 4 are valid for the topologies of Figure 5. The topologies for homogenized material and laminated plate have not been given in the table since they are similar to, and just clearer than, those given in Figures 4-g-i.

Here again it is seen that the rate of convergence for NDER is more than the other approaches. It may be thought that the reason for different rate of convergence lies in the rate of reduction of influence area of the filter as used in (38). Interesting results are obtained when we choose another set of values for reduction of r_0. Here we have used a new reduction steps similar to reduction of mesh size in NDER. For instance we have chosen radius values as

$$r_0 = \sqrt{2}\,a\,h\,,\ a\in\{5,4,2,1\} \tag{39}$$

for a quadrant of a mesh of 40×40 elements. Figure 5 depicts results of the three types of solutions, obtained with SIMP, when either the filter is not used or the rate of reduction of r_0 has been changed according to the new set. It can be seen that although faster convergence is obtained, the topologies obtained are quite different form those given in Figures 4-d-f. This clearly means that the final results are dependent on the path chosen for reduction of the influence area of the filter.

In Figure 6-b, no filter is used in the nodal based approach. The comparison of the figure with Figure 6-c shows that the use of filters in nodal based approach affects the final configuration of the topologies although the convergence is reasonably fast.

The results we have so far presented are for plates with linear behavior. For plates with nonlinear behavior we present the results in Figure 7. The figures show different topologies form those of linear

cases in Figure 4 and 6. One immediate conclusion is that in thin plate theory topologies for linear and nonlinear behaviors are different. In nonlinear behavior, the in-plane actions seem to be dominant and therefore the optimal topologies resemble two bands representing three dimensional truss members.

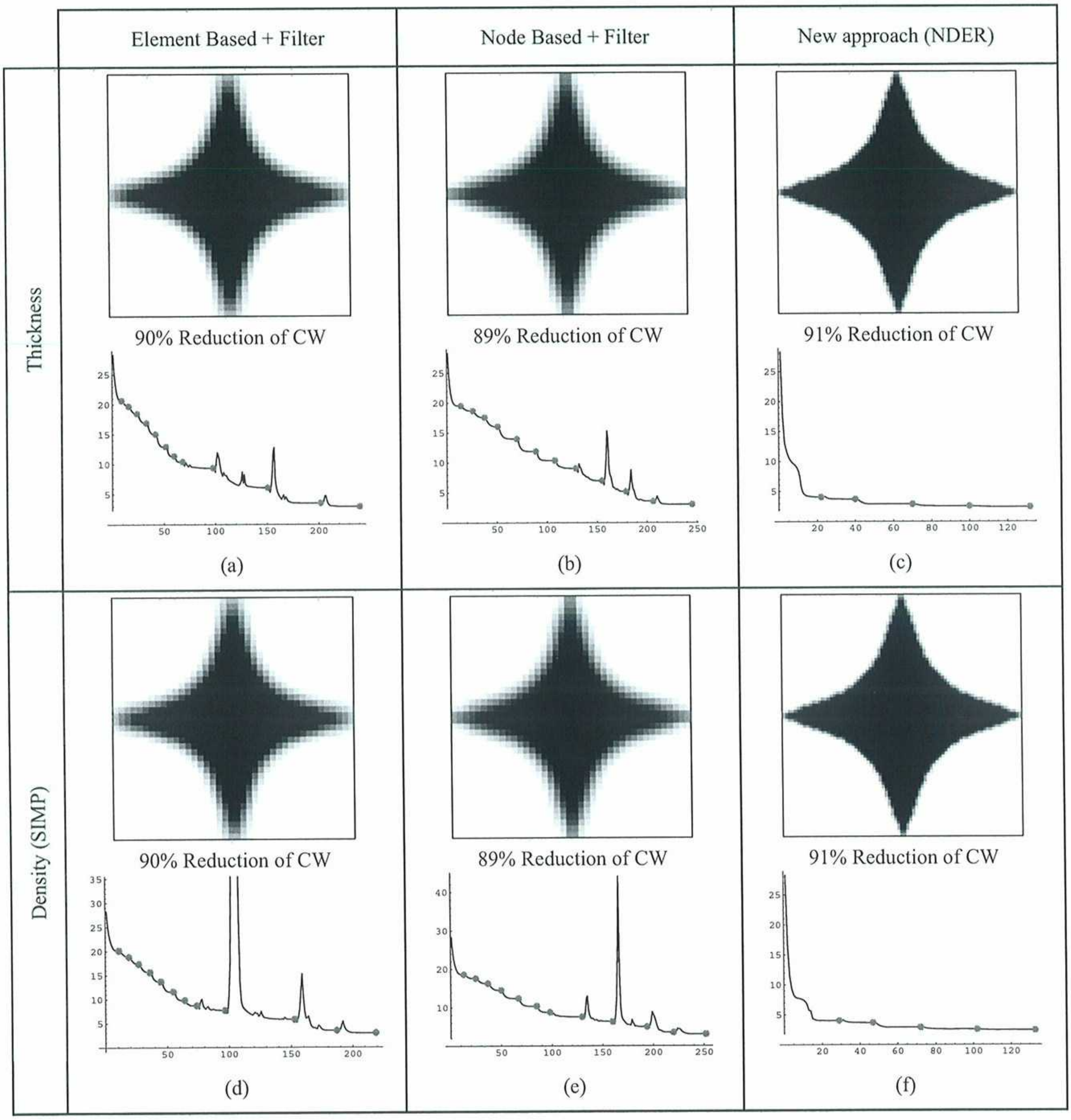

Figure 5. Topologies obtained by different approaches and various choices of design variables for sample problem No.1 when linear behavior is assumed. A mesh of 40×40 square elements is used for finite element solution. Topology and convergence plot for; (a) element based approach using filter and thickness as the design variables, (b) nodal based approach using filter and thickness as the design variables, (c) NDER and thickness as the design variables, (d) element based approach using filter and density, in SIMP method, as the design variables, (e) nodal based approach using filter and density, in SIMP method, as the design variables, (f) NDER and density, in SIMP method, as the design variables.

Unlike the linear cases, convergence is not always obtained by element based approach using thickness as the DV, see Figure 7-a. Also, unlike the linear cases, the topologies with homogenized material,

Figure 7-g-i, are similar to those obtained with thickness and density as DV. The topologies obtained for the laminated plates, Figures 7-j-k, are somewhat similar to those of the linear cases, Figures 4-j-k.

The optimization procedure is performed on a finer mesh for finite element analysis. Figure 8 demonstrates the results. Again no convergence is seen in the element based approach while using thickness as the DV. The results obtained by NDER are similar to those previously presented in Figure 7 and are of high contrast.

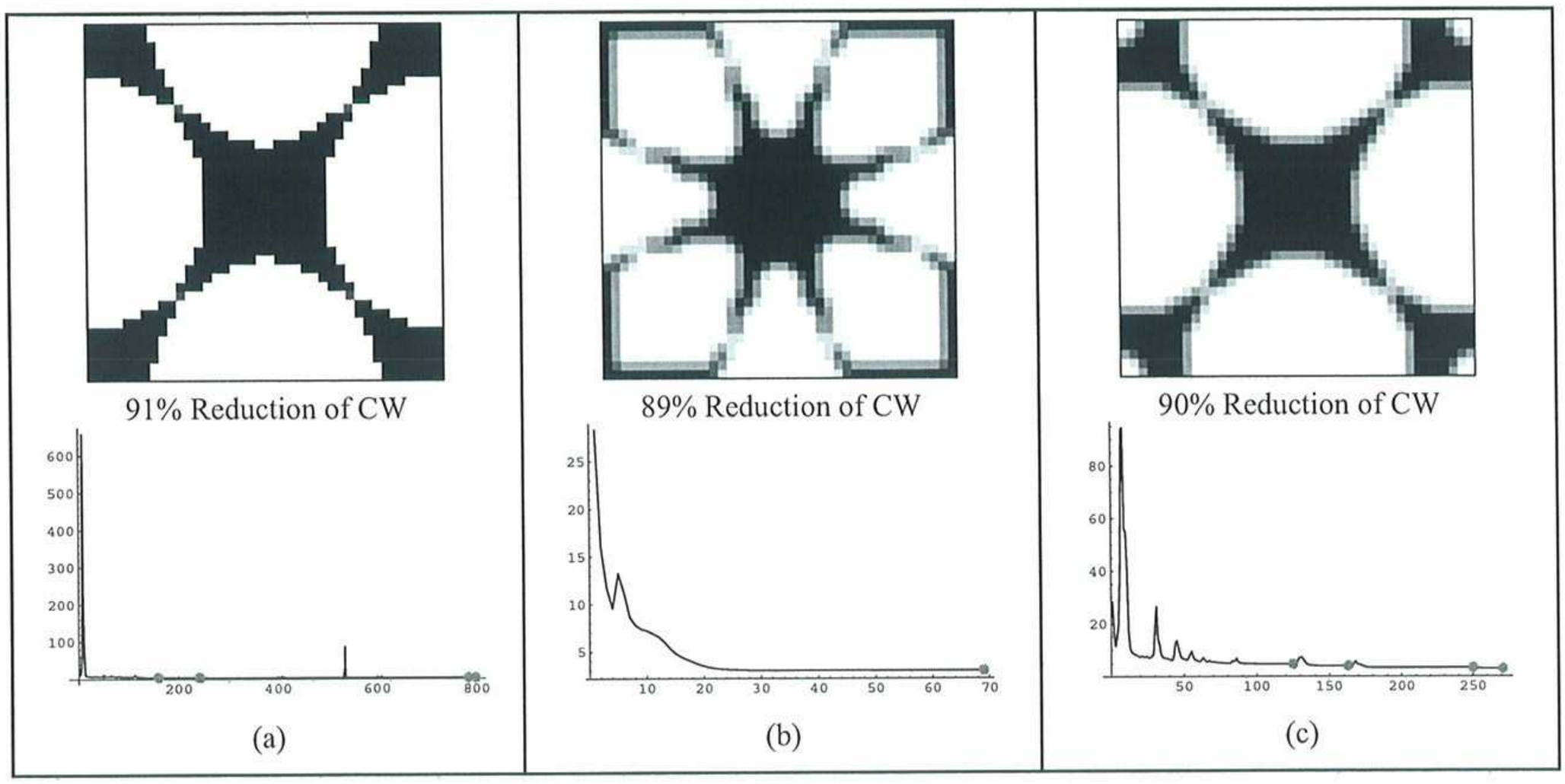

Figure 6. Topologies obtained by SIMP method, (a) element based approach with filter and the new set for r_0 as (39), (b) nodal based approach without filter, (c) nodal based approach with filter and the new set for r_0 as (39).

It might be thought that the reason for the differences in topologies in linear and nonlinear plate behavior lies in the formulation used for the modeling. To investigate such an effect, the optimization procedure is performed again using Mindlin-Reissner hypothesis. Figure 9 shows the result obtained by use of NDER. Note that due to the type of element employed for Mindlin-Reissner formulation, we have not used finer meshes for obtaining clearer topology.

Sample Problem 2. The simply supported plate of the previous problem is now reconsidered with thickness of $t = 150\,mm$. Other geometrical features and mechanical properties of the problem are the same as problem No.1. Here for elastic solutions, a point load of $10\,MPa$ and for nonlinear solution a load of $30\,MPa$ is applied at the center of plate. Again the topology optimization is performed with 30% of the material. The problem is solved with Mindlin-Reissner hypothesis.

All solutions are performed on a mesh of 40×40 square elements for the finite element analysis and due to symmetry of the problem an area of 20×20 elements with a set of appropriate boundary conditions is used. The topologies obtained by NDER are shown in Figure 10. For homogenization approach we have used Model No. 2 (see Figure 1-b).

Interesting to note is that the results for linear and nonlinear solutions are similar. Figure 10 depicts the results for both solutions. Note that, in NDER, we have not used DV meshes finer than $\mathcal{M}_{anal.}$ (see discussion in Section 3.3).

Although not shown, the results of the element and nodal based approaches are similar to those shown

in Figure 10. The main difference between the approaches is the rate of convergence which for NDER is the highest. Figure 11 demonstrates the convergence path of the three approaches. We have also included convergence rate of the solutions with reduction step of r_0 as defined in (39). Unlike the thin plates cases discussed earlier, the final topologies obtained by using Equations (38) and (39), are similar to those shown in Figure 10-b.

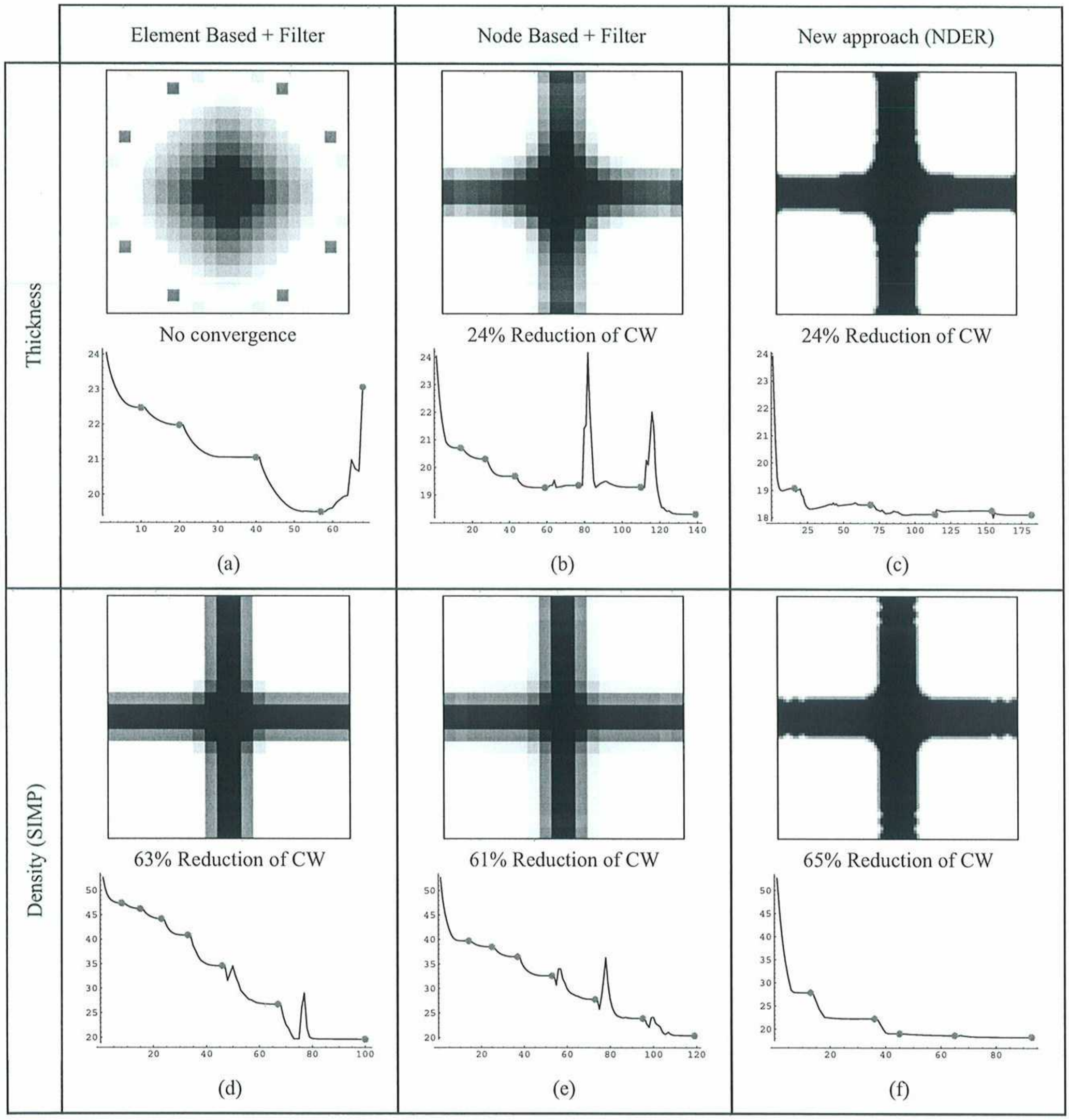

Figure 7. Topologies obtained by different approaches and various choices of design variables for sample problem No.1 when nonlinear behavior is assumed. A mesh of 20×20 square elements is used for finite element solution. Topology and convergence plot for; (a) element based approach using filter and thickness as the design variables, (b) nodal based approach using filter and thickness as the design variables, (c) NDER and thickness as the design variables, (d) element based approach using filter and density, in SIMP method, as the design variables, (e) nodal based approach using filter and density, in SIMP method, as the design variables,

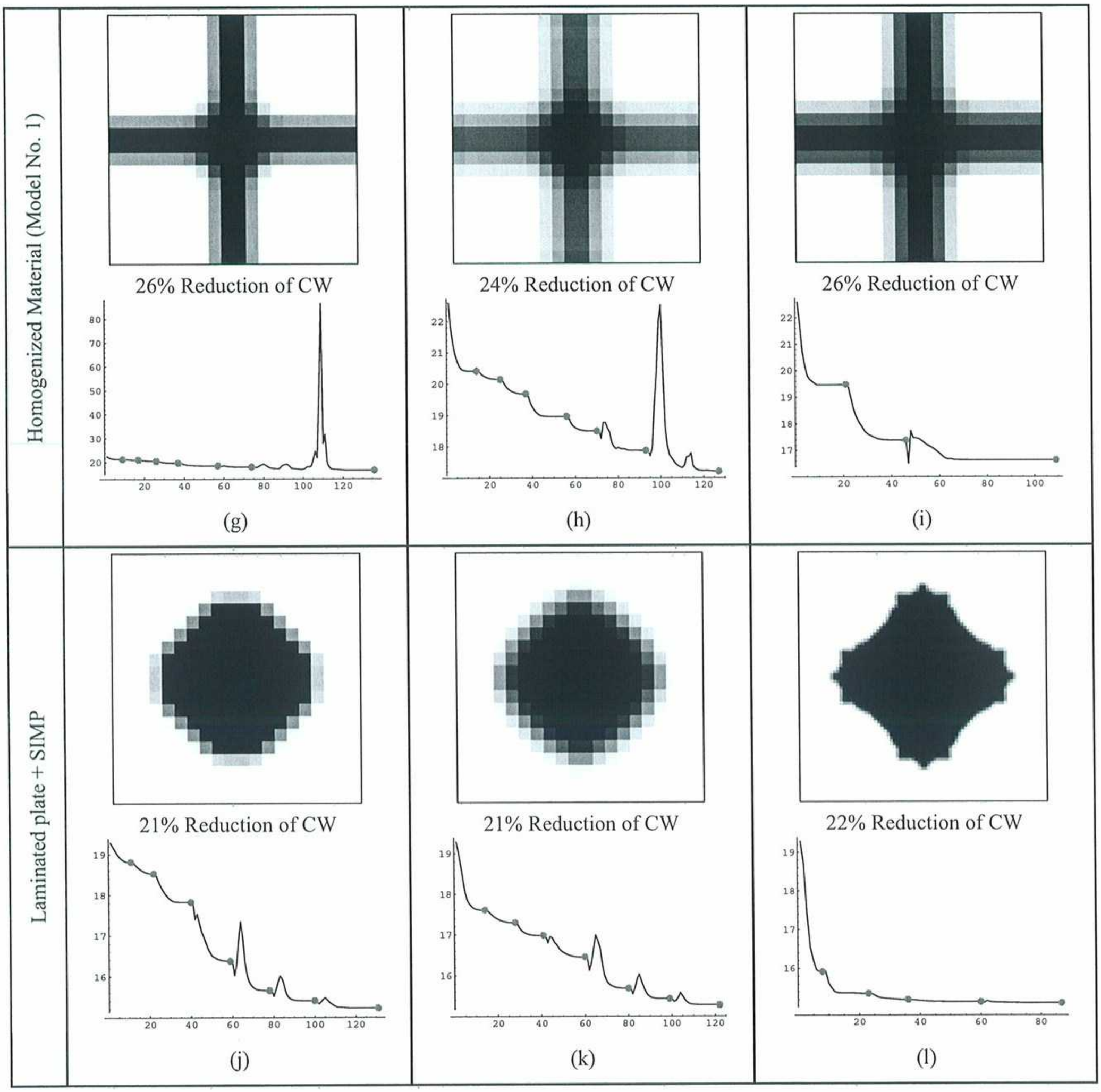

Figure 7. (continued) (f) NDER and density, in SIMP method, as the design variables, (g) element based approach using filter and the equivalent density, in homogenization method with Model No.1, as the design variables, (h) nodal based approach using filter and the equivalent density, in homogenization method with Model No.1, as the design variables, (i) NDER and the equivalent density, in homogenization method with Model No.1, as the design variables, (j) element based approach using filter and density of the top and bottom layers, in SIMP method, as the design variables, (k) nodal based approach using filter and density of the top and bottom layers, in SIMP method, as the design variables, (l) NDER and density of the top and bottom layers, in SIMP method, as the design variables.

This means that the more shear deformation effect is involved the less sensitivity is seen to the rate of r_0 in using filter. The reader may however note that the rate suggested in (39) has been inspired by the mesh sizes in NDER and no information was a priori available for choosing such a form of rate. Although no special tuning has been done for NDER, the results in all studied cases show excellent convergence rate and robustness. This inherently shows that the method we proposed here is very consistence with the finite element solution of plates.

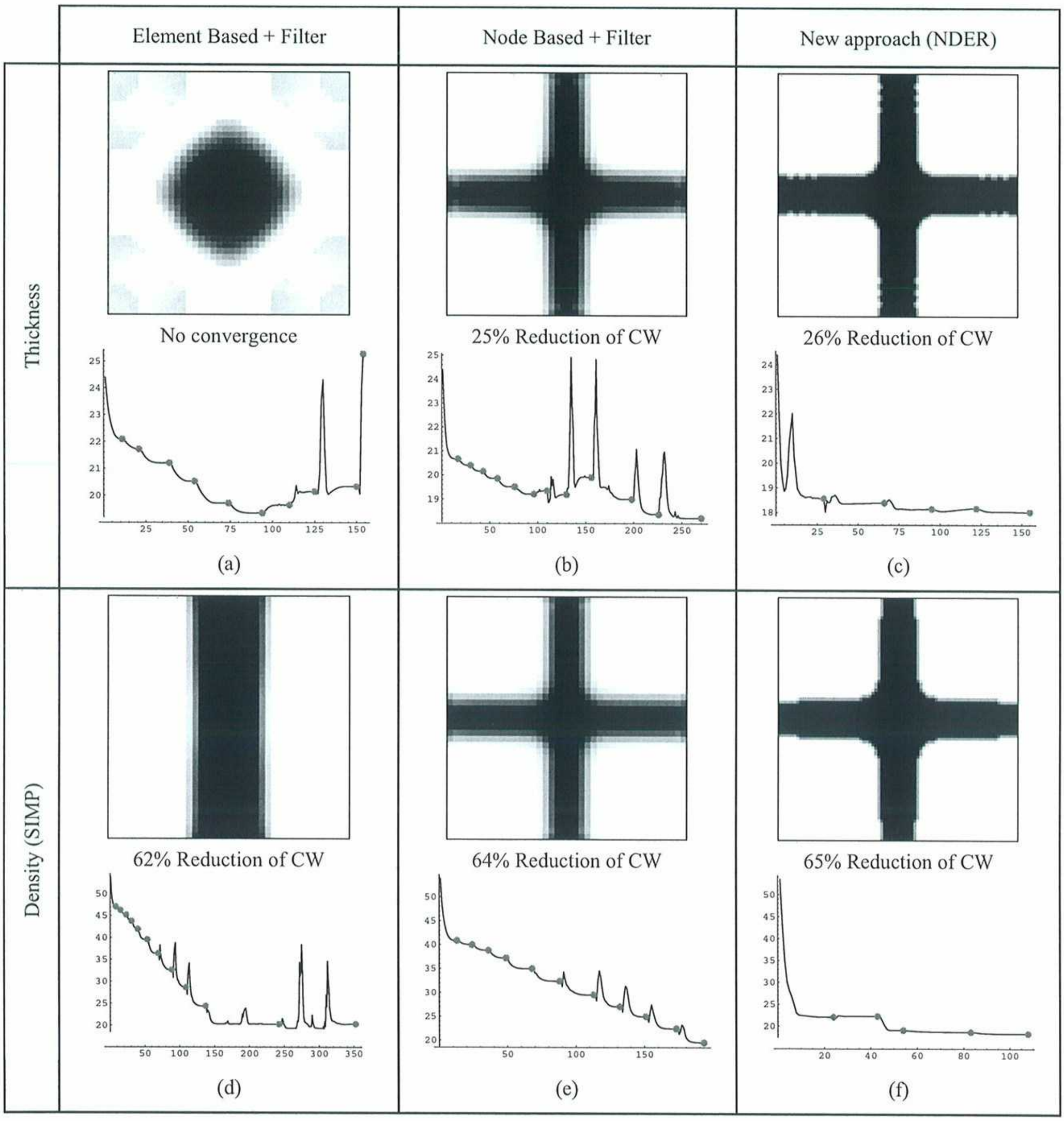

Figure 8. Topologies obtained by different approaches and various choices of design variables for sample problem No.1 when nonlinear behavior is assumed. A mesh of 40×40 square elements is used for finite element solution. Topology and convergence plot for; (a) element based approach using filter and thickness as the design variables, (b) nodal based approach using filter and thickness as the design variables, (c) NDER and thickness as the design variables, (d) element based approach using filter and density, in SIMP method, as the design variables, (e) nodal based approach using filter and density, in SIMP method, as the design variables, (f) NDER and density, in SIMP method, as the design variables.

Sample Problem 3. As the final example we present results of the proposed method for a rectangular plate with one free edge and three simply supported edges (see Figure 3-b). The plate is loaded at the middle of the free edge by a point force. The dimensions of the plate are considered as $L_x = 2\ m$, $L_y = 1\ m$ and $t = 3\ mm$. The mechanical properties are chosen similar to the previous sample problems.

The finite element solution is performed with Kirchhoff hypothesis and the optimization procedure is performed with 70% of material. For $\mathcal{M}_{anal.}$ a grid of 40×20 elements is used and for the $\mathcal{M}_{des.}$, the rule used for the previous examples is followed. The DV are the density of the plate and the laminates (with the use of SIMP method) and just NDER is used for presentation of the results. The $\mathcal{M}_{des.}$ used for the final results is much finer than the $\mathcal{M}_{anal.}$. The final topologies are shown in Figure 12 for linear and nonlinear plate behavior. Significant differences can be seen between the results of linear and nonlinear plate behavior (compare Fig. 12-a and Fig. 12-b with Fig. 12-c and Fig. 12-d, respectively). However, the differences between the results obtained with different DV are not much. This contrasts with the effects seen in sample problem No.1.

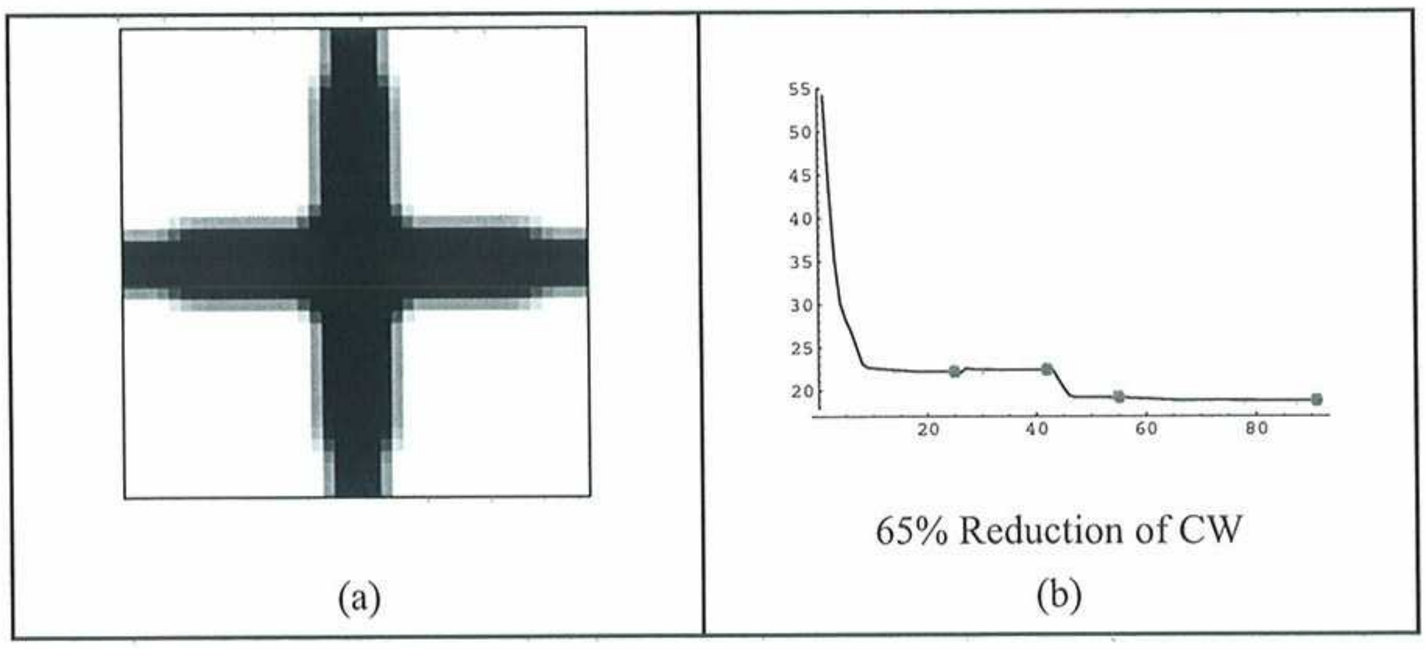

Figure 9. The topology and convergence path obtained for sample problem No. 1, with nonlinear behavior, using Mindlin-Reissner hypothesis. A mesh of 40×40 square elements is used for finite element solution. NDER is used.

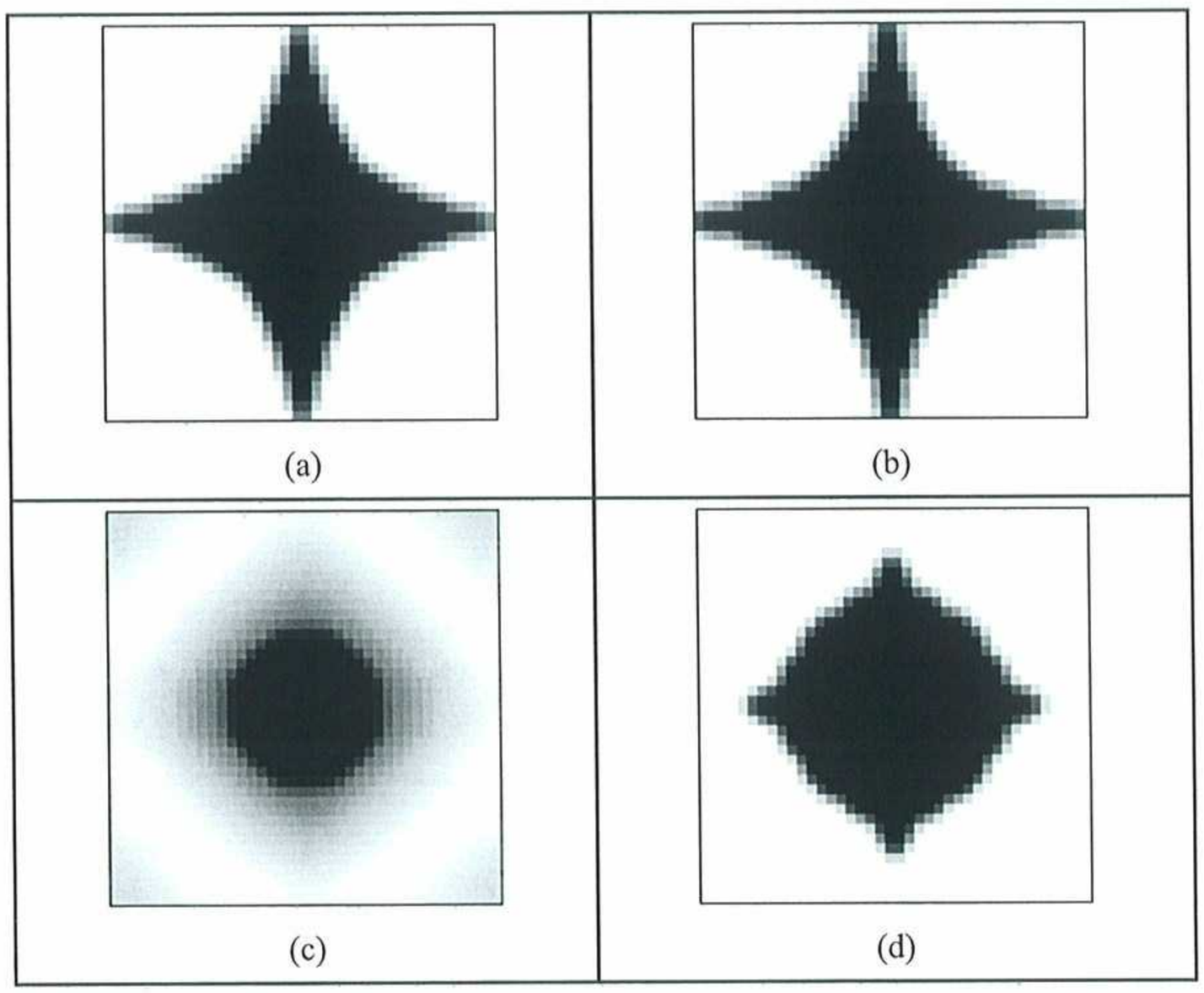

Figure 10. Results of NDER for linear and nonlinear solutions, of the thick plate in sample problem No. 2, with design variables as; (a) thickness (b) density in SIMP method, (c) solid volume in homogenization method with Model No. 2, (d) density of the layers in laminated plate.

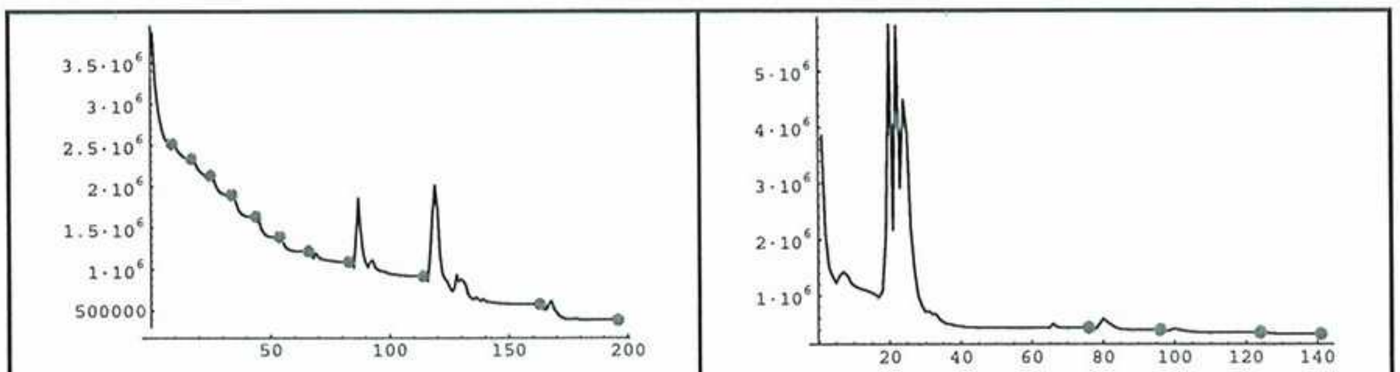

90% Reduction in CW, (with rate of r_0 as Eq. (38))

92% Reduction in CW, (with rate of r_0 as Eq. (39))

(a)

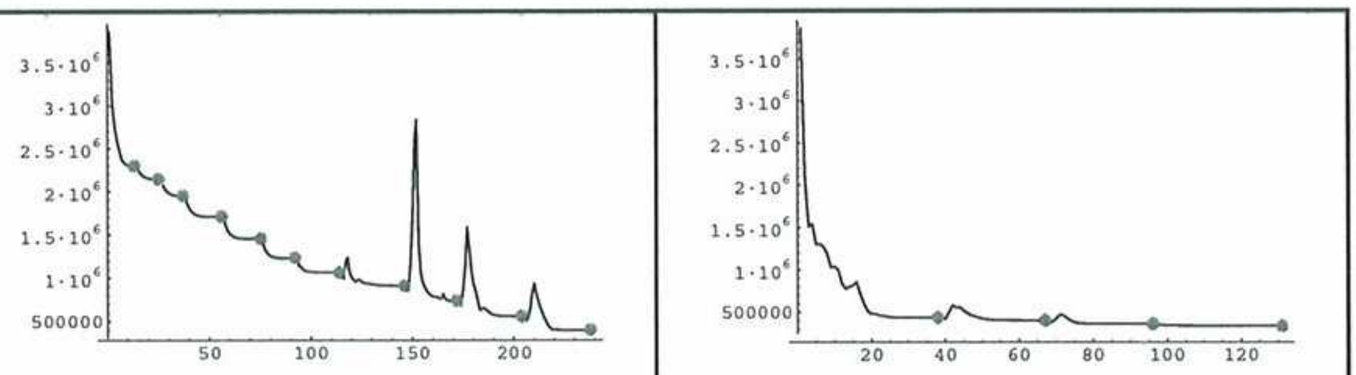

90% Reduction in CW, (with rate of r_0 as Eq. (38))

91% Reduction in CW, (with rate of r_0 as Eq. (39))

(b)

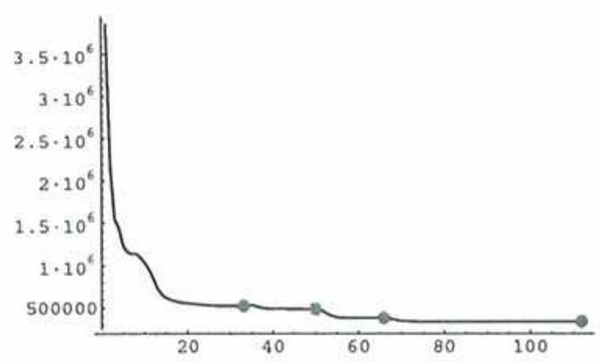

91% Reduction in CW

(c)

Figure 11. Convergence plots for linear solutions - SIMP - Mindlin, (a) Element Based + filter, (b) Nodal Based + filter, (c) NDER

5. CONCLUSIONS

A new continuation has been presented for topology optimization of plate problems. The method is based on sequential mesh refinement for the continuous design variable mesh.

The method has been tested on a wide range of cases. Linear and nonlinear plate behaviors formulated by Kirchhoff and Mindlin-Reissner hypothesis have been considered. Also performance of the method with several choices of design variables has been examined. In each case, the final optimal plate configuration and the convergence of the procedure obtained by NDER have been compared with those obtained by other conventional approaches such as element and nodal based ones.

Main conclusions

The results show that the use of NDER in topology optimization procedure effectively stabilizes the procedure. The method implicitly controls the bounds of the gradients of the design variables in a sequential manner.

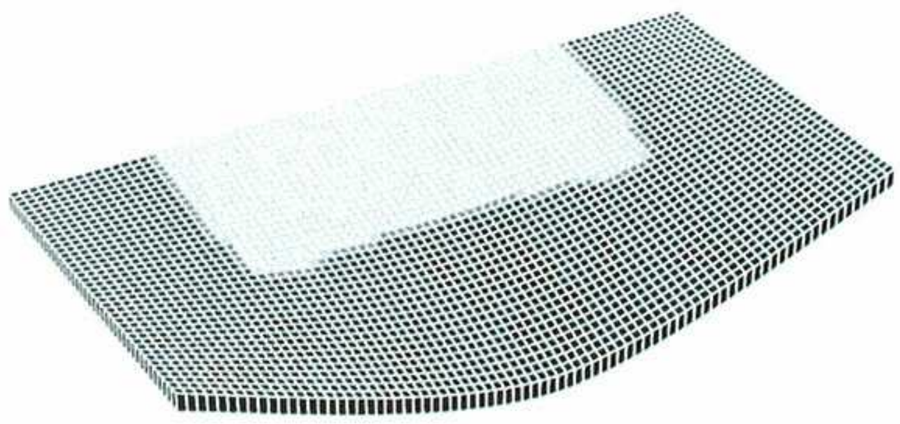

52% Reduction of CW

Linear – layout of stiffeners using NDER

(a)

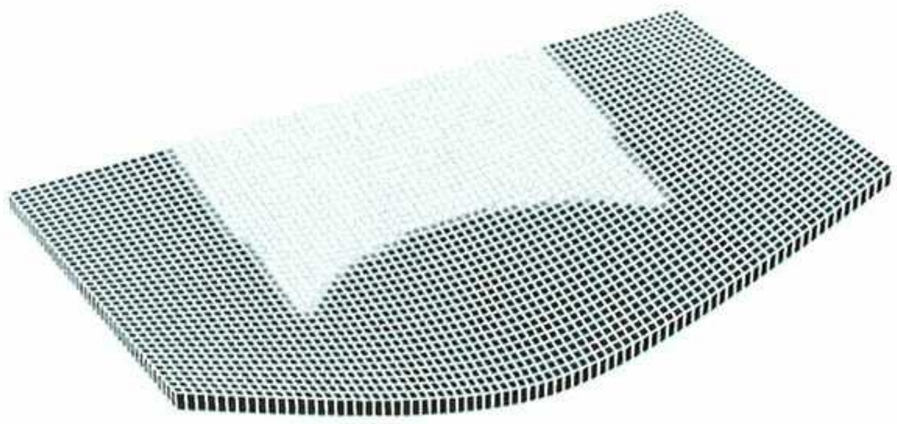

60% Reduction of CW

Linear – SIMP using NDER

(b)

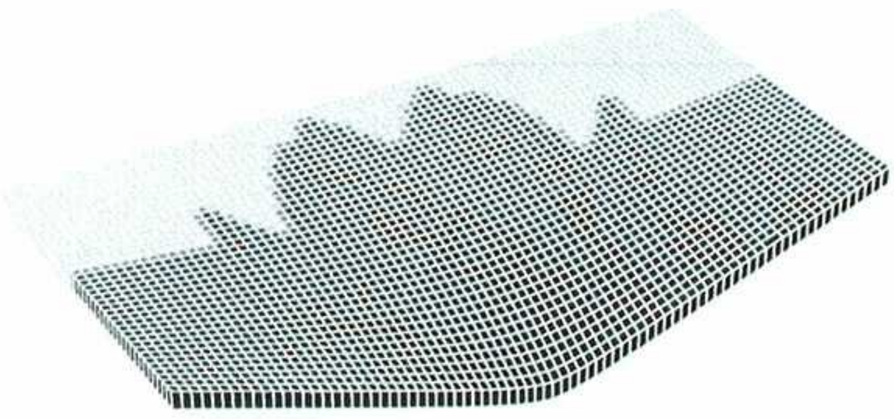

25% Reduction of CW

Nonlinear – layout of stiffeners using NDER

(c)

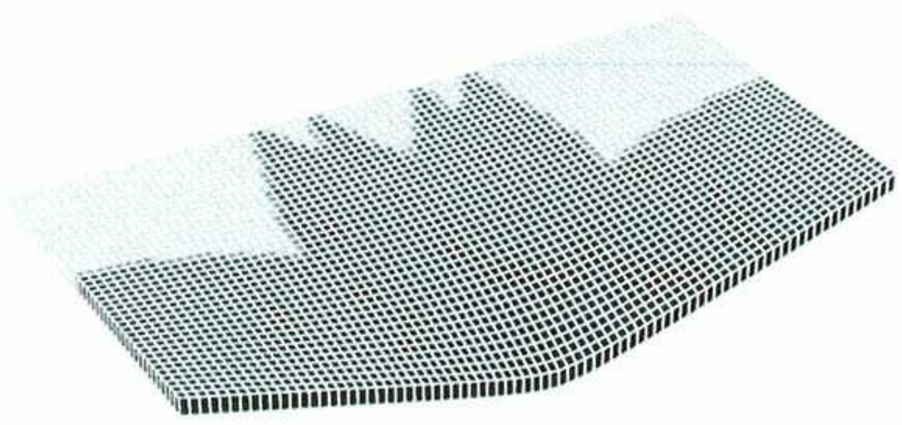

40% Reduction of CW

Nonlinear – SIMP using NDER

(d)

Figure 12. Topologies obtained by the use of NDER for sample problem No.3 shown on the deformed (magnified) configuration. The layout of the material distribution in SIMP method for the plate with; (a) linear behavior and the density of the layers as the DV, (b) linear behavior and its density as DV, (c) nonlinear behavior and the density of the layers as the DV, (d) nonlinear behavior and its density as DV.

Apart from its stabilization effect, the method is capable of giving optimal layouts with more resolution than that of the main mesh used for the FE solution. However, this depends on the formulation used for the modeling of the plate. In using Kirchhoff hypothesis for plate formulation, for the design variables one can easily employ finer meshes compared to that used for FE solution. Our experience shows that for thin plates, formulations with Kirchhoff hypothesis and Mindlin-Reissner hypothesis lead to similar topologies though the paths towards optimal layout are slightly different. This makes NDER more attractive for those who want to obtain more resolution while spending less expense for the FE solution.

Excellent convergence is seen in the results obtained by NDER. The final optimal configurations are mesh-independent. Although this statement does not worth as much as a mathematical proof (that may or may not exist) our experience indicates a superior performance of NDER compared to those of conventional approaches where a sort of instability or mesh dependency is occasionally seen.

Unlike the approaches using filters, NDER dose not need special parameter tuning before the optimization procedure. The method is very consistent with the finite element formulation. This may lead us to find a mathematical base for limits of its application. However, this is beyond the scopes of this report.

Side conclusions

Some complimentary conclusions are as the following;

The results indicate that in thin plates with linear behavior the topologies obtained by the use of thickness and density, as the design variables, are similar. However, the topologies are different from those obtained by homogenization.

It appears that in thin plate formulation with nonlinear behavior the three forms of design variables lead to rather similar topologies.

The results for considering DV as the density of the laminates (stiffeners) are different from those obtained by the three forms mentioned above. However, this conclusion has been drawn just from the solution of a square plate with simply supports. There may be a possibility of obtaining a rather similar results by the forth approach (i.e. DV as the density of the laminates) and the indication has been seen when we changed the square plate to rectangular one with one free edge.

Nevertheless the topologies in linear and nonlinear cases are different. In nonlinear cases the topologies are affected by in-plane actions which are dominant. This in fact affects the convergence of the optimization procedure. In nonlinear plate behavior better convergence is seen compared to linear cases. This may inherently mean that the mesh dependency effect in nonlinear cases is less than that of linear cases (indications are seen in the results of using different rates for change of filer influence area).

In thick plates, the results show that the topologies for linear and nonlinear cases are similar. Also the topologies are similar to those of thin plates with linear behavior. This shows that in nonlinear thick plates, compared to thin plates, bending actions are dominant. In terms of convergence of the solution, thick plates exhibit better behavior than thin plates. Thick plates are less sensitive with respect to rate of change in influence area of filters. Nevertheless, we have shown in this report using NDER reduces almost all sensitivities with respect to convergence of the procedure and as stated before no special parameter tuning is needed as our experience shows.

Final remarks

In this report we have inherently shown that two separate meshes can be used for FE solution and the design variables. Here we have used meshes with similar element types, i.e. both consisting of square elements. It may be possible to use two general meshes for this purpose. In that case, the procedure of refining the mesh of design variables may be performed in an adaptive manner in order to obtain smooth edges for the optimal layout. This, however, can be the subject of the future works.

Acknowledgement

The authors wish to thank Professor K. Svanberg at Department of Mathematics, Royal Institute of Technology, Stockholm, Sweden for generously providing MMA computer program and his helpful guidelines, Professor O. Sigmund at the Technical University of Denmark for valuable discussions, Professor T.J.R. Hughes at University of Texas, Austin, USA, Professor N. Olhoff at Institute of Mechanical Engineering, Aalborg University, Denmark and Professor D.A. Tortorelli at Department of Theoretical and Applied Mechanics, University of Illinois at Urbana Champion, Urbana, USA for their invaluable helps and guidelines. The authors also wish to thank Professor E. Oñate at International Center for Numerical Methods in Engineering (CIMNE), Universidad Politécnica de Cataluña, Spain for his lavish support and encouragement. We also thank Mr. F. Mossaiby at Isfahan University of technology for his kind technical supports during this research.

References

Bendsøe, M.P.; Kikuchi, N. 1988: Generating optimal topologies in optimal design using a homogenization method. *Comput. Meth. Appl. Mech. Engrg.* **71**, 197-224.

Bendsøe, M.P. 1989: Optimal shape design as a material distribution problem. *Struct. Optim.* **1**, 193-202.

Bendsøe, M.P. 1995: *Methods for the optimization of structural topology, shape and material*. Berlin, Heidelberg, New York: Springer.

Bendsøe, M.P.; Guedes, J.M.; Plaxton, S.; Taylor, J.E. 1995: Optimization of structures and material properties for solids composed of softening material. *Int. J. Solids & Struct.* **33**, 1799-1813.

Bendsøe, M.P.; Sigmund, O. 1999: Material interpolation schemes in topology optimization. *Arch. Appl. Mech.* **69**, 635-654.

Boroomand, B.; Zienkiewicz, O.C. 1999: Recovery procedures in error estimation and adaptivity. Part II: adaptivity in nonlinear problems of elasto-plasticity behavior. *Comput. Meth. Appl. Mech. Engrg.* **176**, 127–146.

Bourdin, B. 2001: Filters in topology optimization. *Int. J. Numer. Meth. Engng*, **50**, 2143–2158.

Bruns, T.E.; Tortorelli, D.A. 1998: Topology optimization of geometrically nonlinear structures and compliant mechanism. *Proc. 7-th Symp. on Multidisciplinary Analysis and Optimization,* AIAA/USAF/NASA/ISSMO, AIAA-98-4950, 1874-1882.

Bruns, T.E.; Tortorelli, D.A. 2001: Topology optimization of geometrically nonlinear structures and compliant mechanism. *Comput. Meth. Appl. Mech. Engrg.* **190**, 3443-3459.

Buhl, T.; Pedersen, C.B.W.; Sigmund, O. 2000: Stiffness design of geometrically nonlinear structures using topology optimization. *Struct., Multidisc. Optim.* **19**, 93-104.

Cho, S.; Jung, H.S. 2003: Design sensitivity analysis and topology optimization of displacement-loaded non-linear structures. *Comput. Meth. Appl. Mech. Engrg.* **192**, 2539-2553.

Eschenauer, H.A; Olhoff, N. 2001: Topology optimization of continuum structure: A review. *Appl. Mech. Rev. ASME* **54** (4), 331-389.

Hassani, B.; Hinton, E. 1998: A review of homogenization and topology optimization II- analytical and numerical solution of homogenization equations. *Comput. Struct.* **69**, 719-738.

Haber R.B.; Bendsøe, M.P.; Jog, C. 1996: A new approach to variable-topology shape design using a constraint on the perimeter. *Struct. Optim.* **11**, 1-12.

Hughes, T.J.R.; Cohen M. 1978: The "heterosis" finite element for plate bending. *Comput. Struct.* **9**, 445-450.

Jog, C.S.; Haber, R.B. 1996: Stability of finite element models for distributed-parameter optimization and topology design. *Comput. Meth. Appl. Mech. Engrg.* **130**, 203–226

Jog, C.S. 1997: Distributed-parameter optimization and topology design for nonlinear thermoelasticity. *Comput. Meth. Appl. Mech. Engrg.* **132**, 117-134.

Jones, R.M. 1999: *Mechnics of composite material*, 2nd Edition, London, Taylor & Francis Ltd.

Kemmler, R.; Lipka, A.; Ramm, E. 2005: Large deformations and stability in topology optimization. *Struct., Multidisc. Optim.* **30**, 459-476.

Kim, Y.Y.; Yoon, G.H. 2000: Multi-resolution multi-scale topology optimization- a new paradigm. *Int. J. Solids & Struct.* **37**, 5529-5559.

Lee, S.J.; Bae, J.E.; Hinton, E. 2000: Shell topology optimization using the layered artificial material model. *Int. J. Numer. Meth. Engng.* **47**, 843-867.

Matsui, K.; Terada, K. 2004: Continuous approximation of material distribution for topology optimization. *Int. J. Numer. Meth. Engng.* **59**, 1925–1944.

Maute, K.; Ramm, E. 1997: Adaptive topology optimization of shell structures. *AIAA J.* **35**, 1767–1773.

Maute, K; Schwarz, S.; Ramm, E. 1998: Adaptive topology optimization of elastoplastic structures. *Struct. Optim.* **15**, 81-91.

Niordson, F.I. 1983: Optimal design of plates with a constraint on the slope of the thickness function. *Int. J. Solids & Struct.* **19**, 141-151.

Pedersen, C.B.W.; Buhl, T.; Sigmund, O. 2001: Topology synthesis of large-displacement compliant mechanisms. *Int. J. Numer. Meth. Engrg.* **50**, 2683-2705.

Pedersen, N.L. 2001: On topology optimization of plates with prestress. *Int. J. Numer. Meth. Engrg.* **51**, 225-239.

Petersson, J. 1999: Some convergence results in perimeter-control topology optimization. *Comput. Meth. Appl. Mech. Engrg.* **171**, 123-140.

Petersson, J.; Sigmund, O. 1998: Slope constrained topology optimization. *Int. J. Numer. Meth. Engng.* **41**, 1417-1434

Peric, D.; Hochard, Ch.; Dutko, M.; Owen, D.R.J. 1996: Transfer operators for evolving meshes in small strain. *Comput. Meth. Appl. Mech. Engrg.* **137**, 331-344.

Rahmatalla, S.; Swan, C.C. 2003: Continuum Topology Optimization of Buckling-Sensitive Structures. *AIAA Journal,* **41**, 1180-1189.

Rahmatalla, S.F.; Swan, C.C. 2004: A Q4/Q4 Continuum Structural Topology Optimization Formulation. *Struct. Multidisc. Optim.* **27**, 130-135.

Rozvany, G.I.N.; Zhou, M. 1991: Application of COC method in layout optimization. In: Eschenauer, H.; Mattheck, C.; Olhoff, N. (eds.) *Proc. Conf. "Eng. Opt. in Design Process"* (held in Karlsruhe 1990), 59-70. Berlin, Heidelberg, New York: Springer-Verlag.

Rozvany, G.I.N. 2001: Aims, scope, methods, history and unified terminology of computer–aided topology optimization in structural mechanics. *Struct. Multidisc. Optim.* **21**, 90-108.

Sigmund, O. 1994: *Design of material structures using topology optimization.* Ph.D. Thesis, Department of Solid Mechanics, Technical University of Demark.

Sigmund O. 1997: On the design of compliant mechanisms using topology optimization. *Mech. Struc. & Mach.* **25**(4), 493-524.

Sigmund, O.; Petersson, J. 1998: Numerical instabilities in topology optimization: A survey on procedures dealing with checkerboard, mesh-dependencies and local minima. *Struct. Optim.* **16**, 68-75.

Simo, J.C.; Fox, D.D. 1989: On a stress resultant geometrically exact shell model. Part I: Formulation and optimal parameterization. *Comput. Meth. Appl. Mech. Engrg.* **72**, 267-304.

Stegmann, J.; Lund, E. 2005: Nonlinear topology optimization of layered shell structures. *Struct., Multidisc. Optim.* **29**, 349-360.

Stoer, J.; Bulirsch, R. 1993: *Introduction to numerical analysis,* 2nd. Edition, Springer-Verlag.

Stolpe, M.; Stidsen, T. 2006: A hierarchical method for discrete structural topology design problems with local stress and displacement constraints. *Int. J. Numer. Meth. Engng*, (in press).

Svanberg, K. 1987: The method of moving asymptotes- A new method for structural optimization. *Int. J. Numer. Meth. Engrg.* **24**, 359-373.

Swan, C.S.; Kosaka, I. 1997: Voigt-Reuss Topology optimization for structures with non-linear material behaviors. *Int. J. Numer. Meth. Engrg.* **40**, 3785-3814.

Tenek, L.H.; Hagiwara, I. 1993: Optimization of material distribution within isotropic and anisotropic plates using homogenization. *Comput. Meth. Appl. Mech. Engrg.* **109**, 155-167.

Vanderplaates, G.N., 1985: *Numerical optimization techniques for engineering design*. McGraw-Hill.

Xie Y.M.; Steven G.P. 1993: A simple evolutionary procedure for structural optimization. *Comput. Struct.* **49**, 885-896.

Zhou, M.; Shyy, Y.K.; Thomas, H.L. 2001: Checkerboard and minimum member size control in topology optimization. *Struct., Multidisc. Optim.* **21**, 152-158.

Zienkiewicz, O.C.; Cheung, Y.K. 1964: The finite element method for analysis of elastic isotropic and orthotropic slabs. *Proc. Inst. Civ. Eng.* **28**, 471-488.

Zienkiewicz, O.C.; Taylor, R.L. 2000: *The Finite Element Method*, 5th Edition, Stoneham, MA, Butterworth-Heineman.

List of figures

List of tables